MCB
Journals.ASM.org

# $Na^+/H^+$ Exchanger 1 Directly Binds to Calcineurin A and Activates Downstream NFAT Signaling, Leading to Cardiomyocyte Hypertrophy

**Takashi Hisamitsu, Tomoe Y. Nakamura, and Shigeo Wakabayashi**

Department of Molecular Physiology, National Cerebral and Cardiovascular Center Research Institute, Suita, Osaka, Japan

**The calcineurin A (CaNA) subunit was identified as a novel binding partner of plasma membrane $Na^+/H^+$ exchanger 1 (NHE1). CaN is a $Ca^{2+}$-dependent phosphatase involved in many cellular functions, including cardiac hypertrophy. Direct binding of CaN to the $^{715}$PVITID$^{720}$ sequence of NHE1, which resembles the consensus CaN-binding motif (PXIXIT), was observed. Overexpression of NHE1 promoted serum-induced CaN/nuclear factor of activated T cells (NFAT) signaling in fibroblasts, as indicated by enhancement of NFAT promoter activity and nuclear translocation, which was attenuated by NHE1 inhibitor. In neonatal rat cardiomyocytes, NHE1 stimulated hypertrophic gene expression and the NFAT pathway, which were inhibited by a CaN inhibitor, FK506. Importantly, CaN activity was strongly enhanced with increasing pH, so NHE1 may promote CaN/NFAT signaling via increased intracellular pH. Indeed, $Na^+/H^+$ exchange activity was required for NHE1-dependent NFAT signaling. Moreover, interaction of CaN with NHE1 and clustering of NHE1 to lipid rafts were also required for this response. Based on these results, we propose that NHE1 activity may generate a localized membrane microdomain with higher pH, thereby sensitizing CaN to activation and promoting NFAT signaling. In cardiomyocytes, such signaling can be a pathway of NHE1-dependent hypertrophy.**

Maintenance of intracellular pH ($pH_i$) is critical for the function of most enzymes, membrane proteins, and organic and inorganic molecules. The $pH_i$ is strictly regulated by a combination of various acid and base transporters, including the acid-extruding transporter $Na^+/H^+$ exchanger 1 (NHE1), a ubiquitously expressed isoform of the NHE family of countertransport proteins (38, 44, 56). NHE1 is a dimer that consists of 2 heterocomplexes of the transporter protein with a cytosolic subunit, calcineurin B (CaNB) homologous protein (CHP), an essential cofactor preserving the structure and function of NHE1 (1, 17, 34, 36). The NHE1 molecule is comprised of 2 major domains—an N-terminal ion transport domain with transmembrane helices and a regulatory C-terminal cytoplasmic domain that associates with signaling molecules (50). NHE1 is activated in response to various stimuli, including hormones, growth factors, and mechanical stress (50), which often lead to increased disease pathogenesis, e.g., heart failure and cancer (6, 22).

Since the initial identification and cloning of NHE1 (43), many studies have focused on the molecular mechanism underlying its regulation, and several regulatory proteins and bioactive lipids that interact with the C-terminal domain of NHE1 have been identified. For example, we recently reported that hormonal activation of NHE1 may be mediated by the direct interaction of diacylglycerol with the lipid-interacting domain of NHE1 (48). Activation of NHE1 results in elevations of $pH_i$ and the $Na^+$ concentration, which regulates a variety of physiological and pathological processes. However, how activation of NHE1 promotes downstream signaling via specific NHE1-interacting molecules is poorly understood.

To provide insight into the NHE1-dependent signaling pathway, we first aimed to identify novel binding partners of NHE1 by using a combination of affinity purification and mass spectrometry (MS). As a result, we identified calcineurin (CaN) as a novel NHE1-binding protein. CaN is a $Ca^{2+}$-dependent serine/threonine protein phosphatase, which is a heterodimeric complex of a 58- to 64-kDa catalytic A subunit and a 19-kDa regulatory B subunit (7, 27). In mammals, the A subunit has 3 isoforms (α, β, and γ), and the B subunit has 2 isoforms (CaNB1 and -B2). Unlike CaNAγ, CaNAα and CaNAβ are widely expressed in various tissues and regulate a variety of cellular processes, including the immune response, neurotransmitter release in the brain, and muscle hypertrophy (42). Upon elevation of intracellular $Ca^{2+}$ levels, the binding of $Ca^{2+}$-calmodulin (CaM) complex to the CaM-binding domain in the CaNA subunit increases its enzymatic activity by releasing the autoinhibitory domain blocking the active site (7, 27). Nuclear factors of activated T cells (NFAT) transcription factors are the best-characterized substrates of CaN (7, 19, 27, 33). After dephosphorylation by CaN, cytosolic NFAT subunits (NFATc1 to NFATc4) are translocated into the nucleus, where they increase the transcription of many genes. Some CaN is known to be associated with the plasma membrane which may then interact with multiple membrane proteins (26, 54). In fact, several reports suggest CaN-dependent regulation of membrane proteins, such as ligand-gated or voltage-gated ion channels (54). Conversely, it is not well understood how CaN is activated at the plasma membrane of cells through specific target molecules.

In cardiomyocytes, activation of CaN-NFAT signaling is one of the major $Ca^{2+}$-dependent prohypertrophic pathways (15, 35). Activation of NHE1 is also involved in cardiac hypertrophy and heart failure, as shown by studies in animal models and isolated cardiomyocytes (10, 12, 21, 37, 53). The expression level of NHE1 was reported to be elevated in various hypertrophic animal models (12, 24). Furthermore, we recently reported that, based on

Received 31 January 2012 Returned for modification 24 February 2012
Accepted 5 June 2012
Published ahead of print 11 June 2012
Address correspondence to Shigeo Wakabayashi, wak@ri.ncvc.go.jp.

doi:10.1128/MCB.00145-12

results using transgenic mice with activated NHE1, activation of NHE1 is sufficient for increasing prohypertrophic $Ca^{2+}$ signals, leading to cardiac hypertrophy and heart failure (37). Therefore, the identification of CaN as an NHE1-binding partner prompted us to investigate whether the NHE1-CaN interaction plays a pathological role in the genesis of cardiomyocyte hypertrophy.

In the present study, we demonstrate that CaN directly interacts with the specific site of the NHE1 cytoplasmic domain and amplifies downstream NFAT signaling, thereby enhancing gene expression and leading to cardiomyocyte hypertrophy.

## MATERIALS AND METHODS

**Reagents.** Thrombin, methyl-β-cyclodextrin (MβCD), and FK506 were purchased from Sigma. Ionomycin was obtained from Calbiochem. The following antibodies were used: rabbit anti-NHE1 (3), mouse anti-NHE1 (BD Transduction Laboratory), rat antihemagglutinin (anti-HA) (Roche), rabbit anti-pan-CaNA (Cell Signaling Technology), rabbit anti-CaNB (Santa Cruz Biotechnology), rabbit anti-phospho-protein kinase A RII (anti-phospho-PKA RII) monoclonal antibody (Epitomics), mouse anti-flottilin-1 (BD Biosciences), mouse anti-α-actinin (Sigma), mouse anti-glyceraldehyde-3-phosphate dehydrogenase (anti-GAPDH) (Millipore), rabbit anti-atrial natriuretic factor (anti-ANF) (Abcam PLC), and mouse anti-RCAN1 (ABNOVA). The anti-CaNA and -CaNB antibodies used in this study did not cross-react with CHP1. A peptide (14-mer) corresponding to residues $^{711}$KEDLPVITIDPASP$^{724}$ of NHE1 and control peptides GPHPVIVITGPHEE and GPHPVIAVNGPHEE were synthesized to >95% purity (Invitrogen). All other chemicals employed were of the highest available purity.

**Molecular biology.** The plasmid carrying the cDNA for human NHE1 contained some unique restriction sites, which were cloned into the pECE mammalian expression vector as described previously (49). A PCR-based strategy was performed to construct insertion or deletion mutant cDNA, as previously reported (49), by using a template plasmid encoding NHE1 tagged with hemagglutinin (HA; amino acid sequence, PYDVPDYA) at its C terminus, which was designated NHE1-HA (18). For construction of NHE1 incorporating extracellular HA tags, 2 tandem HA tags and glycine linkers consisting of 25 amino acids (GGYPYDVPDYAGGGYPYDVPDYAGG) were inserted between amino acids (aa) 281 and 282 of NHE1, which was designated NHE1-2HA. To construct NHE1 tagged with a peptide derived from the CaN-specific substrate RII (designated NHE1*-RIIpep-HA), NHE1 was truncated after aa 760 by using a PCR-based strategy and then connected to aa 85 to 103 of human RIIα (GenBank accession no. NP_004148). The PCR fragments were sequenced with a Perkin-Elmer ABI model 3130 autosequencer. To generate an expression vector for the human CaNAα, CaNAβ, and CaNB1 subunits, each cDNA was purchased from Invitrogen and cloned into pcDNA3.1(−) or pcDNA3.1/Hygro(−) (Invitrogen) mammalian expression vectors. Human NFATc1 and mouse NFATc4 clones were purchased from Open Biosystems and cloned into the pEGFP-N1 vector to generate green fluorescent protein (GFP) fusion proteins.

**Adenovirus production.** PCR fragments were produced from NHE1-2HA, the NHE1 mutant (Δ715–720), or NFATc4-GFP and cloned into the entry vector (pDONR221) by Gateway technology (Invitrogen). Subsequently, inserts in the resulting vectors were transferred into the destination vector (pAd/CMV/V5-DEST) according to the manufacturer's protocol (Invitrogen). These adenovirus expression vectors were transfected into HEK293A cells, and adenovirus carrying the genes of interest was produced for about 10 days according to the manufacturer's protocol (Invitrogen). The titer of adenoviruses was measured with an adenovirus titer immunoassay kit (Cell Biolabs, Inc.). Titers ranged from $5 \times 10^8$ to $5 \times 10^9$ PFU/ml.

**Cell culture, DNA transfection, and adenovirus infection.** An $Na^+/H^+$ exchanger-deficient cell line (PS120) (40) and its transfectants were maintained in Dulbecco's modified Eagle's medium (DMEM; Sigma-Aldrich) supplemented with 25 mM $NaHCO_3$, 7.5% (vol/vol) fetal calf serum, penicillin (50 U · $ml^{-1}$), and streptomycin (50 μg · $ml^{-1}$) at 37°C in the presence of 5% $CO_2$. PS120 cells ($5.0 \times 10^5$ cells per 100-mm dish) were transfected with each NHE1 plasmid construct (10 μg) by using a calcium phosphate coprecipitation technique. Cells that stably expressed mutant NHE1 were selected using the "$H^+$-killing" technique (47). Transfection with plasmids carrying CaNAα plus CaNB1 or CaNAβ plus CaNB1 was performed using Lipofectamine 2000 (Invitrogen), and the resultant stable cell lines were selected with 1 mg · $ml^{-1}$ G418 plus 0.2 mg · $ml^{-1}$ hygromycin. The transport-deficient mutant E262I was transfected into PS120 cells, and stable cell lines were selected with G418.

Primary culture of neonatal rat ventricular myocytes from 1- to 3-day-old Sprague-Dawley rats was essentially carried out as described previously (37). Cardiomyocytes were plated on laminin-coated glass-bottom dishes and maintained in DMEM supplemented with 10% fetal calf serum, L-glutamine, and penicillin-streptomycin. Two days later, myocytes were transfected overnight with plasmids carrying NHE1-2HA or the NHE1 Δ715–720-2HA deletion mutant by using Lipofectamine 2000 under serum-free conditions. Subsequently, myocytes were infected at a multiplicity of infection (MOI) of ~100 with adenovirus carrying NFATc4-GFP, and FK506 (1 μM) was added to some dishes. For experiments examining the hypertrophic response, myocytes were similarly infected with adenovirus carrying NHE1-2HA or the Δ715–720-2HA deletion mutant. As a control experiment, some cells were stimulated with phenylephrine (PE; 10 μM). Two days later, cells were subjected to immunoblotting or confocal microscopy.

**Identification of NHE1-binding proteins by LC-MS/MS analysis.** PS120 cells that stably expressed HA-tagged or untagged wild-type NHE1 were plated onto 20 500-$cm^2$ dishes and grown to confluence (a total of $4.0 \times 10^9$ cells). Cells were solubilized for 20 min on ice with 200 ml of lysis buffer (150 mM NaCl, 0.1 mM $CaCl_2$, 20 mM HEPES [pH 7.2]), 1% Triton X-100, and Complete EDTA-free protease inhibitor cocktail (Roche) and were then centrifuged at 27,000 × *g* for 20 min. Subsequently, the supernatant was incubated for 1 h at 4°C with Sepharose CL-4B (GE Healthcare UK, Ltd.) to remove proteins that bound nonspecifically to the resin. The adsorbed supernatant was incubated with 1 ml anti-HA affinity matrix (Roche) at 4°C for 2 h. The beads were washed twice with 10 ml lysis buffer, twice with 10 ml high-salt lysis buffer (lysis buffer with 500 mM NaCl), and once with 10 ml low-detergent lysis buffer (lysis buffer with 0.1% Triton X-100). Proteins that specifically bound to the anti-HA beads were eluted in 1 ml sodium dodecyl sulfate-polyacrylamide gel electrophoresis (SDS-PAGE) sample buffer (Invitrogen). SDS-PAGE was performed on a 4 to 12% NuPAGE gradient gel (Invitrogen), and the protein bands were visualized using a silver stain mass spectrometry (MS) kit (Wako Pure Chemical Industries, Ltd.).

For liquid chromatography-tandem mass spectrometry (LC-MS/MS) analysis, the bands of interest were excised and then trypsinized in the gel at 35°C for 20 h. The sample was separated by high-performance liquid chromatography (Magic 2002; Michrom BioResources, Inc.) on a Magic $C_{18}$ column (Michrom BioResources, Inc.). MS data were obtained using a Q-TOF II system (Waters Micromass), and the isolated proteins were identified by searching the National Center for Biotechnology Information nonredundant sequence database with the Mascot search engine (Matrix Science). LC-MS/MS analyses were performed by the APRO Life Science Institute, Inc. (Tokushima, Japan).

**Expression and purification of constitutively activated CaN.** Constitutively activated CaN (CA-CaN) was expressed as a complex of a glutathione *S*-transferase (GST)-fused human CaNAα mutant (aa 1 to 398) lacking the CaM-binding and autoinhibitory domains with full-length human CaNB1 (aa 1 to 170) in *Escherichia coli* BL21 Star(DE3) cells (Invitrogen), as described previously (41). The protein complex was induced with isopropyl-β-D-thiogalactopyranoside (IPTG) and purified with glutathione-Sepharose (GE Healthcare), and the GST tag was removed by digestion with PreScission protease (GE Healthcare) according to the manufacturer's protocol. The digested protein complex was further purified by gel filtration using prep-grade HiLoad 16/60 Superdex 200 (GE

Healthcare). The final eluate was concentrated to 1.1 mg · $ml^{-1}$ and analyzed by SDS-PAGE and Coomassie staining.

**Pulldown assay.** cDNA encoding the C-terminal domain (aa 503 to 815) of human NHE1 was cloned into the pMal-c vector (New England BioLabs, Inc.). Recombinant proteins fused with maltose binding protein (MBP) were expressed in BL21 Star(DE3) cells. Bacterial cells from 500 ml of culture were sonicated and centrifuged, and the supernatant was applied to an amylose resin column equilibrated with phosphate-buffered saline (PBS) and incubated for 30 min at room temperature. The resin was washed 3 times with PBS, and a mixture of recombinant human CaN (A and B complex; 5.8 μg) (Biomol), 500 μg bovine testes CaM (Sigma), and 0.2 mM $CaCl_2$ was added to the resin. In one experimental series, protein extract from bacteria expressing CaNB without CaNA was subjected to a pulldown assay. To examine the competitive effect of CaN-binding peptides, CA-CaN (7.8 μg) was incubated with the indicated concentration of 14-mer synthesized peptides, and the mixture of CA-CaN and each peptide was applied to the protein-bound amylose resin. After incubation for 1 h at 4°C, the resin was washed 4 times with PBS, and bound proteins were eluted with PBS containing 10 mM maltose and analyzed by SDS-PAGE.

**Measurement of $^{22}Na^+$ uptake and $pH_i$.** The $^{22}Na^+$ uptake activity and its dependence on $pH_i$ were measured by using the $pH_i$ clamp method (20). Briefly, cells in 24-well plates were depleted of serum for more than 5 h and preincubated for 30 min at 37°C in $Na^+$-free choline chloride-KCl medium containing 20 mM HEPES-Tris (pH 7.4), 1.2 to 140 mM KCl, 2 mM $CaCl_2$, 1 mM $MgCl_2$, 5 mM glucose, and 5 μM nigericin. Subsequently, $^{22}Na^+$ uptake was initiated by the addition of choline chloride-KCl solution containing $^{22}NaCl$ (37 kBq · $ml^{-1}$; 1 mM final concentration), 1 mM ouabain, and 100 μM bumetanide. In some wells, the uptake solution contained 0.1 mM 5-(*N*-ethyl-*N*-isopropyl)amiloride (EIPA; Molecular Probes). After 1 min of $Na^+$ uptake, the cells were rapidly washed 4 times with ice-cold PBS to terminate the reaction. The $pH_i$ was calculated on the basis of the imposed $[K^+]$ gradient by assuming the equilibrium intracellular $[K^+]$/extracellular $[K^+]$ $([K^+]_i/[K^+]_o) = [H^+]_i/[H^+]_o$ and a $[K^+]_i$ of 120 mM. The data were normalized with respect to the protein concentration, which was measured using a bicinchoninic assay kit (Pierce Chemicals) and bovine serum albumin (BSA) as a standard.

The change in $pH_i$ induced by various extracellular agents was measured by using the $[^{14}C]$benzoic acid equilibration method in serum-deprived cells (47). The $pH_i$ was also measured using the dual-excitation ratiometric pH indicator BCECF-AM (Invitrogen), as previously described (17). Briefly, the fluorescence was measured at 510 to 530 nm with alternating excitations at 440 and 490 nm through a 505-nm dichroic reflector. Images were collected every 5 s using a cooled charge-coupled device (CCD) camera (ORCA-ER; Hamamatsu Photonics K.K., Japan) mounted on an inverted microscope (IX 71; Olympus) with a 20× objective (UAPO/340; Olympus) and processed with AQUACOSMOS software (Hamamatsu Photonics). The $pH_i$ was calibrated using a high-$[K^+]$ solution containing 140 mM KCl, 2 mM $CaCl_2$, 1 mM $MgCl_2$, and 5 μM nigericin and adjusted to pH values of between 6.0 and 8.0 with a mixture of MES (morpholineethanesulfonic acid) and HEPES.

**Measurement of CaN activity *in vitro*.** The phosphatase activity of CaN was determined using a CaN assay kit (Biomol) with slight modification of the manufacturer's instructions. Briefly, recombinant human CaN (Biomol) was incubated with the CaN substrate protein kinase A (PKA) regulatory subunit phospho-RII peptide in 20 mM HEPES, 20 mM MES (adjusted to pH 6.3 to 9.1 with Tris), 100 mM NaCl, 6 mM $MgCl_2$, 0.5 mM dithiothreitol (DTT), 0.025% NP-40, 0.5 mM $CaCl_2$, and 0.25 μM CaM for 30 min at room temperature, and the amount of released phosphate was measured. To determine the $Ca^{2+}$ dependency of CaN activity, the solution contained a constant concentration (0.1 mM) of $CaCl_2$ and various concentrations of EGTA, which was added to produce various free $Ca^{2+}$ concentrations ($10^{-9}$ to $10^{-5}$ M) at different pH values calculated by the Cabuf program (G. Droogmans, KU Leuven, Leuven, Belgium). The data were fitted to a Hill equation with the aid of a simulation program (Graph Pad Prism).

**Promoter assay.** The transcriptional activity of NFAT was measured using the Dual-Glo luciferase assay system (Promega). Cells that expressed wild-type and mutant NHE1 were plated on a 96-well plate ($2.0 \times 10^4$ cells · $well^{-1}$). After 24 h, the cells were transfected with 90 ng of pGL4.30[luc2P/NFAT-RE/Hygro] and 10 ng of pGL4.75[hRluc/CMV] vectors per well under serum-free conditions for 24 h. The former plasmid contains the firefly luciferase gene and the NFAT response element, which is the promoter region of the interleukin-2 gene, while the latter is an expression control vector. The cells were stimulated with 10% serum with or without 3 mM MβCD or 1 μM FK506 for 17 h, and the luminescence was measured using a Luminous CT-9000D (Dia-Iatron) luminometer. The luminescence of luc2P, which indicated promoter activity, was normalized to that of hRluc.

**Coimmunoprecipitation and immunoblotting.** For coimmunoprecipitation, cells were washed with ice-cold PBS and solubilized in lysis buffer for 20 min on ice. After centrifugation for 5 min at 16,000 × *g*, the supernatant was incubated with protein A-Sepharose beads (Pierce) supplemented with the indicated antibodies for 2 h at 4°C. Subsequently, the beads were washed 5 times with ice-cold lysis buffer and proteins were eluted with SDS-PAGE sample buffer (Invitrogen) containing 50 mM dithiothreitol. After SDS-PAGE on 4 to 12% NuPAGE gradient gels (Invitrogen), the proteins were transferred electrophoretically onto polyvinylidene fluoride membranes and subjected to immunoblotting with the indicated antibodies. The immunoblotted proteins were visualized using an enhanced chemiluminescence detection system (Nacalai Tesque, Japan).

**Sucrose density gradient centrifugation.** Cells grown on 100-mm dishes were treated for 17 h with 3 mM MβCD. Control or MβCD-treated cells were homogenized in 1.1 ml of ice-cold lysis buffer containing 0.1% Triton X-100, 50 mM NaCl, 0.1 mM $CaCl_2$, and 50 mM Tris-HCl (pH 7.6) with protease inhibitors. The lysate was sonicated 5 times for 5 s with 30-s intervals on ice and then incubated for 60 min at 4°C. The sucrose concentration of the lysate was adjusted to 45% by mixing with concentrated sucrose solution, and the resulting solution (2.5 ml) was placed at the bottom of the tubes. Subsequently, 2.5 ml and 2 ml of a 35% sucrose solution and 5% sucrose solution, respectively, containing 50 mM NaCl, 0.1 mM $CaCl_2$, and 50 mM Tris-HCl (pH 7.6) were layered to produce a discontinuous sucrose gradient with a total volume of 7 ml, and sample tubes were centrifuged by the Hitachi ultracentrifuge (himac; CS150GXII) at 196,000 × *g* for 17 h at 4°C with a swing rotor (Hitachi; S50ST). The fractions were divided into 10 samples (700 μl each). Samples were analyzed by SDS-PAGE and immunoblotting.

**Confocal microscopy.** Fibroblastic cells on glass-bottom dishes were washed twice with PBS, fixed with Mildform fixative (Wako, Japan) for 10 min, and permeabilized with PBS containing 0.1% Triton X-100 for 3 min. The cells were then treated for 60 min with rat anti-HA (1:100), rabbit anti-RII (pSer96) (1:100), or rabbit anti-pan-CaNA antibodies (1:100) in PBS with 5% BSA. In some experiments (see Fig. 7A and 9A), cells were stained after fixation (without permeabilization) with anti-HA antibody. Subsequently, cells were fluorescently stained with Alexa Fluor 488- or Alexa Fluor 546-labeled secondary antibodies (1:400). The fluorescence of double-labeled cells was analyzed with a laser scanning confocal attachment (FluoView FV1000; Olympus Corp.) on an inverted microscope (IX81; Olympus) equipped with an oil immersion objective (60×, 1.42 numerical aperture; PlanApoN [Olympus]). Immunostaining and confocal microscopy of cardiomyocytes were performed by essentially the same method used for fibroblasts. Following immunostaining, cardiomyocytes were incubated for 2 min with DAPI (4′,6-diamidino-2-phenylindole) for nuclear staining.

The localization of ganglioside GM1, a marker of lipid rafts, was observed in cells that expressed NHE1-HA by using a Vybrant lipid raft labeling kit (Invitrogen). Briefly, cells were labeled at 4°C with Alexa Fluor 488-conjugated cholera toxin subunit B, which binds to GM1. The cells

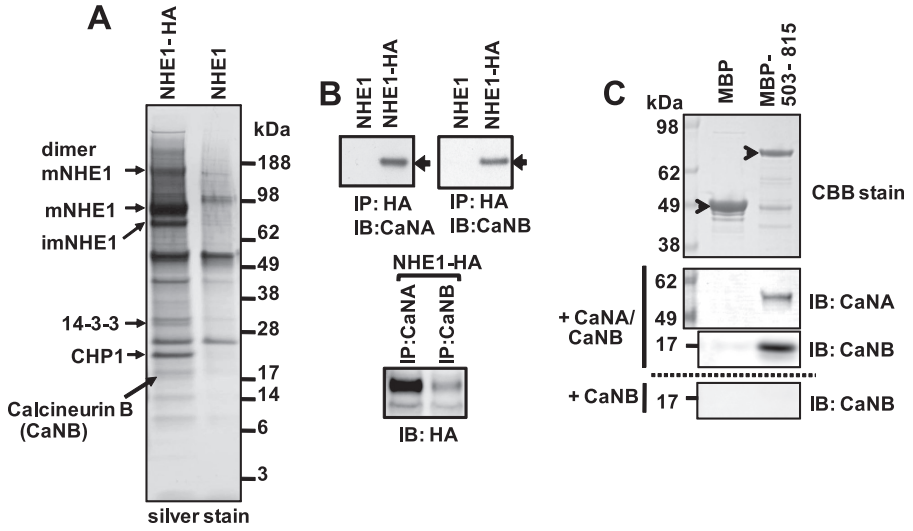


**FIG 1** Identification of CaN as a novel binding partner of NHE1. (A) Affinity purification of lysates from cells expressing HA-tagged or untagged NHE1 was performed as described in Materials and Methods. In addition to the known NHE1 binding partners, CHP1 and 14-3-3, we demonstrated that the B subunit of CaN (CaNB) copurifies with NHE1. mNHE1, mature (fully glycosylated) NHE1; imNHE1, immature (core-glycosylated) NHE1. (B) Coimmunoprecipitation of cells expressing NHE1-HA or untagged NHE1 with the indicated antibodies, which were used for immunoprecipitation (IP) and immunoblotting (IB). CaNA and CaNB were coprecipitated with NHE1-HA. (C) Pulldown assay with MBP or MBP fusion proteins containing the C-terminal domain of NHE1 (aa 503 to 815). MBP or fusion proteins were visualized by Coomassie brilliant blue (CBB) staining (upper panel). Recombinant CaNA/CaNB complex (middle panels) or cell lysates of *E. coli* expressing CaNB without CaNA (lower panel) was applied to the resin, and the gel was analyzed by IB with the indicated antibodies.

were then fixed, permeabilized, and stained with rat anti-HA (1:100) and Alexa Fluor 546-conjugated secondary antibodies (1:400) at 4°C. Finally, the cells were analyzed by confocal microscopy.

For observation of the subcellular localization of NFAT in fibroblasts, cells were transfected with enhanced GFP (EGFP)-labeled human NFATc1 (hNFATc1-GFP) in medium supplemented with 10% serum. One day later, the medium was depleted of serum for 3 to 10 h. In some experiments (for nuclear export), cells were continuously incubated in serum-supplemented medium. Fields (8 to 20 positions) that include cells showing nuclear or extranuclear localization of NFAT were selected on the microscope equipped with a stage controller. Cells were stimulated with various agents in the presence or absence of inhibitors. Fifteen to 60 min later, the same fields before addition of agents were again observed with the confocal microscope. For analysis of overall subcellular localization of NFAT, cells were fixed and the fluorescence intensity of GFP in the nucleus and cytosolic regions was measured using a confocal system equipped with imaging software, and the nucleus/cytosol ratio was calculated to indicate the nuclear translocation of NFAT. For observation of the subcellular localization of NFAT in cardiomyocytes, cells were transfected with plasmids carrying extracellular HA-tagged NHE1 variants and subsequently infected with adenovirus carrying hNFATc4-GFP under serum-free conditions. Two days later, myocytes were fixed and immunostained with anti-HA antibody, followed by Alexa Fluor 546-labeled secondary antibody for detection of sarcolemmal expression of NHE1 variants. Nuclear localization of NFAT in cardiomyocytes was analyzed similarly as in fibroblasts.

**Statistical analysis.** Data were expressed as the means ± standard deviations (SD) of at least 3 determinations. We used the unpaired Student's *t* test for comparison between 2 groups and one-way analysis of variance followed by the Dunnett's test for comparison of more than 2 groups. *P* values of $<0.05$ were considered statistically significant.

## RESULTS

**CaN is a novel binding partner of NHE1.** To identify novel proteins that interact with NHE1, we performed large-scale affinity purification of HA-tagged NHE1 and analyzed proteins that coprecipitated with NHE1 by using LC-MS/MS. We isolated the NHE1-HA protein complex (~100 μg) and identified candidate binding partners that were only present in the lysate from NHE1-HA transfectants and not in that from untagged NHE1 transfectants (Fig. 1A). In addition to CHP1 (31) and 14-3-3 (29), we found that calcineurin B (CaNB) copurifies with NHE1 (Fig. 1A). As CaN is a heterodimer that is comprised of the CaNA/B complex, we predicted that CaNA would also interact with NHE1. While this interaction could not be detected in a silver-stained gel since the CaNA band overlaps that of other proteins (data not shown), both CaNA and CaNB subunits coprecipitated with NHE1-HA and vice versa (Fig. 1B), suggesting that the CaNA/B complex interacts with NHE1. Furthermore, both CaNA and CaNB were pulled down by the cytosolic C-terminal domain of NHE1 (aa 503 to 815) fused with MBP, but not by MBP alone (Fig. 1C). Next, we addressed which subunits of CaN would directly interact with NHE1. A similar pulldown assay using only CaNB (without CaNA) and the NHE1 C terminus resulted in no detection of CaNB in the pulldown eluent (Fig. 1C, bottom panel), indicating that CaNB is not directly bound to NHE1. However, CaNA could not be tested alone because CaNB is required for its structural stability. Thus, these data suggest that CaNA directly interacts with the C-terminal domain of NHE1, while CaNB indirectly associates with NHE1 through CaNA.

**CaN directly binds to the $^{715}$PVITID$^{720}$ sequence in the C-terminal domain of NHE1.** To identify the CaN-binding site in the C-terminal domain of NHE1, we performed coimmunoprecipitation assays using cells that expressed HA-tagged NHE1 C-terminal domain deletion mutants (Fig. 2A). Deletions of the NHE1 C terminus before residue 709 abolished its coprecipitation with CaN, while deletion of the C-terminal 65 residues (Δ750-HA) preserved its interaction with CaN (Fig. 2A), suggesting that aa 709 to 750 of NHE1 are necessary for the interaction of NHE1 with CaN. Sequence analysis of this region revealed a 6-residue motif ($^{715}$PVITID$^{720}$) that is similar to the CaNA-binding motif

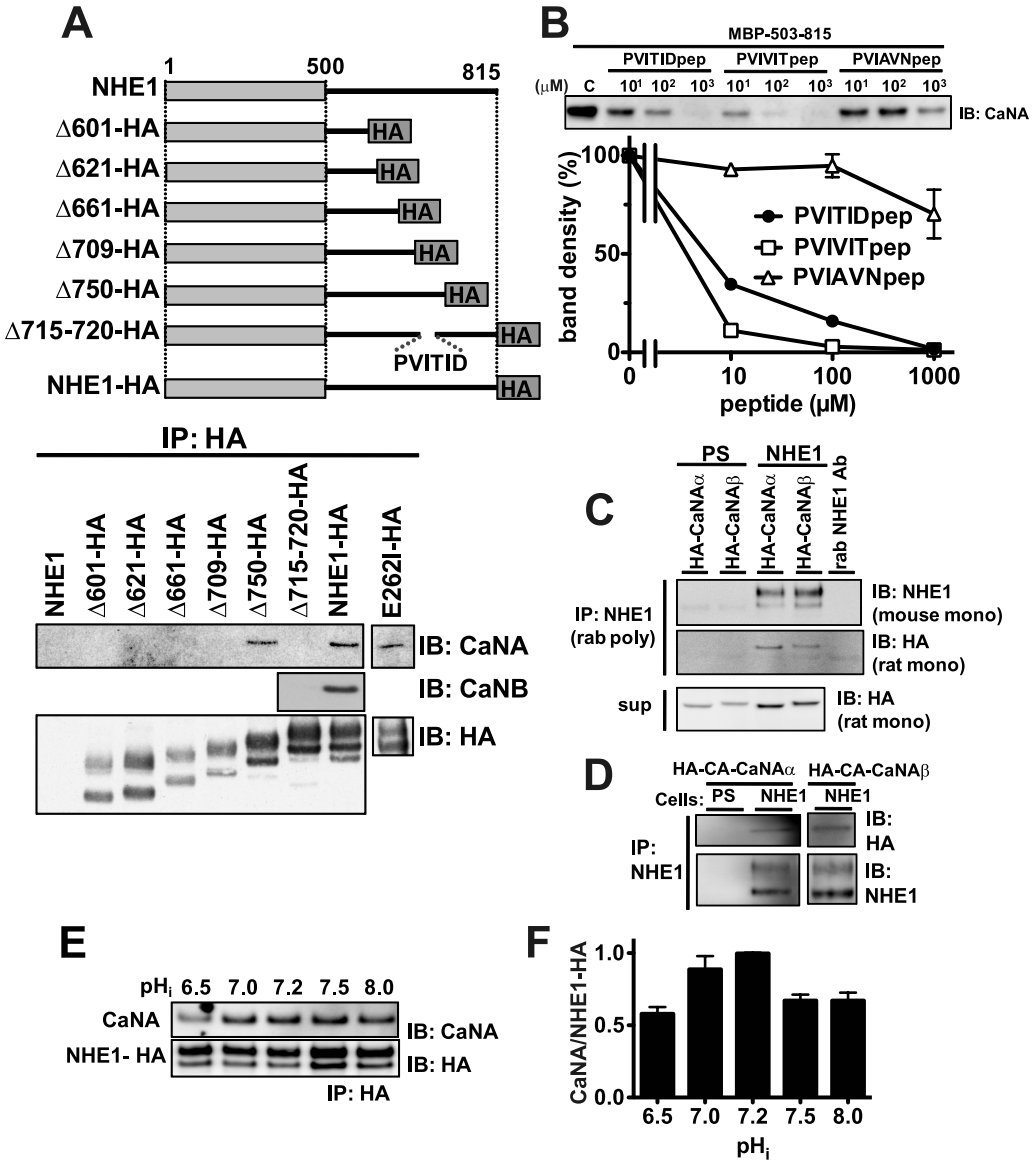


**FIG 2** Identification and characterization of the CaN-binding site in the NHE1 C terminus. (A) Schematic representation of C-terminal deletion mutants of HA-tagged NHE1 (upper panel). Lysates from cells that expressed each mutant were immunoprecipitated with an anti-HA antibody and then immunoblotted with anti-pan-CaNA or anti-HA antibodies (lower panel). The upper and lower bands in the HA immunoblot correspond to the fully glycosylated mature and the core-glycosylated immature forms of NHE1-HA, respectively. (B) Effect of peptides on the interaction between CaN and NHE1. A pulldown assay of CaN was performed in the presence of an NHE1-derived peptide (0 to 1 mM) containing PVITID or 2 other control sequences (PVIVIT, model CaN-binding motif; PVIAVN, weakly interacting control sequence) (30). Relative band density (% of control [lane C]) was plotted against the peptide concentrations. Data ($n = 3$) are shown as means ± SD (lower panel). For this experiment, a recombinant constitutively active form of CaN (CA-CaN) was used. (C) Both CaNAα and CaNAβ interact with NHE1. Untransfected (PS) or NHE1-transfected cells were transiently transfected with CaNB1 and HA-CaNAα or HA-CaNAβ, and the cell lysates were coimmunoprecipitated with the indicated antibodies (Ab). The cell lysate input (sup) is also shown. The rightmost lane shows the negative control using the antibody alone (1 μg). rab, rabbit; poly, polyclonal antibody; mono, monoclonal antibody. (D) Similar experiments were also performed in PS120 cells (PS) or NHE1 transfectants that expressed HA-tagged CA-CaNAα or CA-CaNAβ. (E) Effect of $pH_i$ for NHE1-CaN interaction. Cells expressing HA-tagged NHE1 were placed for 30 min in the buffer containing 140 mM KCl and 5 μM nigericin to clamp the $pH_i$ at various values. CaNA and NHE1-HA proteins were detected by immunoblotting after immunoprecipitation with anti-HA antibody. (F) The amount of coprecipitated CaNA was represented after normalization with that of NHE1-HA. Data ($n = 3$) are shown as means ± SD.

(PXIXIT, where X is any amino acid) present in the NFAT transcription factor and other known CaN-interacting proteins (see Fig. 11B) (2). Indeed, deletion of these 6 residues (Δ715–720) prevented the coprecipitation of both CaNA and CaNB with NHE1-HA (Fig. 2A), indicating that the interaction between CaN and NHE1 is mediated by this motif but not other regions of NHE1. To confirm that this region represents the CaN-binding site of NHE1, we synthesized a short 14-mer peptide containing the PVITID sequence and examined whether it could inhibit the pulldown of CaN by the C-terminal domain of NHE1. Incubation with the NHE1-derived peptide (PVITIDpep) markedly inhibited the pulldown of CaN (50% inhibitory concentration [$IC_{50}$], ~10

μM) (Fig. 2B). Moreover, another peptide containing the PVIVIT sequence, reported as a high-affinity CaN-binding peptide (30), inhibited the pulldown even more effectively ($IC_{50}$, ≤10 μM). In contrast, a peptide containing the PVIAVN sequence, reported to weakly interact with CaN (30), had a marginal effect on the pulldown (Fig. 2B). These data suggest that the PVITID sequence of NHE1 is the binding site for the A subunit of CaN.

We also examined the isoform specificity of the interaction of CaNA with NHE1. Both HA-tagged CaNAα and CaNAβ subunits, cotransfected with CaNB in NHE1-expressing cells, were coprecipitated with NHE1 (Fig. 2C). Moreover, the constitutively active (CA)-CaNA subunits—lacking the CaM-binding and autoinhibitory domains—also bound to NHE1 (Fig. 2D), indicating that these regulatory domains are not required for the interaction of CaNA with NHE1. These results are consistent with the previous finding that peptides containing the PXIXIT consensus sequence interact with the catalytic domain of CaNA (30).

We next addressed the $pH_i$ dependence of the interaction between NHE1 and CaNA in cells. Cells expressing HA-tagged NHE1 were incubated with high $K^+$ and nigericin buffer at various pHs to clamp $pH_i$, and then NHE1-HA was immunoprecipitated with anti-HA antibody (Fig. 2E). The amount of coprecipitated CaNA was normalized to that of NHE1 (Fig. 2F). These data indicate that CaNA can bind to NHE1 at a wide range of $pH_i$ values, although the interaction appears to be slightly reduced at acidic and alkaline $pH_i$ values.

**NHE1 activates the CaN/NFAT signaling pathway.** CaN dephosphorylates NFAT, which promotes the nuclear translocation of NFAT and stimulates transcription of various genes driven by an NFAT-specific promoter (7). Therefore, we examined whether the interaction of NHE1 with CaN modulates the CaN/NFAT pathway. A control experiment was first conducted to confirm that the expression of either CA-CaNAα or CA-CaNAβ (together with CaNB) resulted in a 4- to 5-fold increase in NFAT transcriptional activity (shown by an increase in luciferase reporter activity versus untransfected cells), an activation that was completely inhibited by a CaN inhibitor, FK506 (Fig. 3A). Interestingly, overexpression of wild-type NHE1 in PS120 cells lacking endogenous NHE1 also significantly increased luciferase activity in the presence of serum (Fig. 3B). Enhanced luciferase activity was also observed in CCL39 cells (parental cell line of PS120) expressing the endogenous NHE1 (Fig. 3B). These data indicate that NHE1 amplifies the CaN/NFAT signaling pathway. However, the effect of NHE1 was marginal when cells were maintained under serum-free conditions (Fig. 3C), suggesting that activation of NHE1 in response to serum may potentiate NHE1-induced NFAT signal activation.

Next, we addressed whether NHE1 potentiates nuclear translocation of NFAT. NHE1 transfectants were transiently transfected with GFP-tagged NFATc1 and then serum deprived. Cells showing extranuclear localization of NFAT were initially selected, exposed to various agents, and then observed on a confocal microscope (Fig. 4A). Treatment with the $Ca^{2+}$ ionophore ionomycin, which is expected to maximally activate cellular CaN, resulted in nuclear translocation of NFAT in all cells observed (Fig. 4A and B). Incubation (1 h) in serum-supplemented medium promoted nuclear translocation of NFAT in 11 out of 41 cells in NHE1 transfectants, but not in untransfected PS120 cells (Fig. 4B). Such translocation was inhibited by the CaN inhibitor FK506 and the NHE1 inhibitor EIPA (Fig. 4B). These results suggest that the

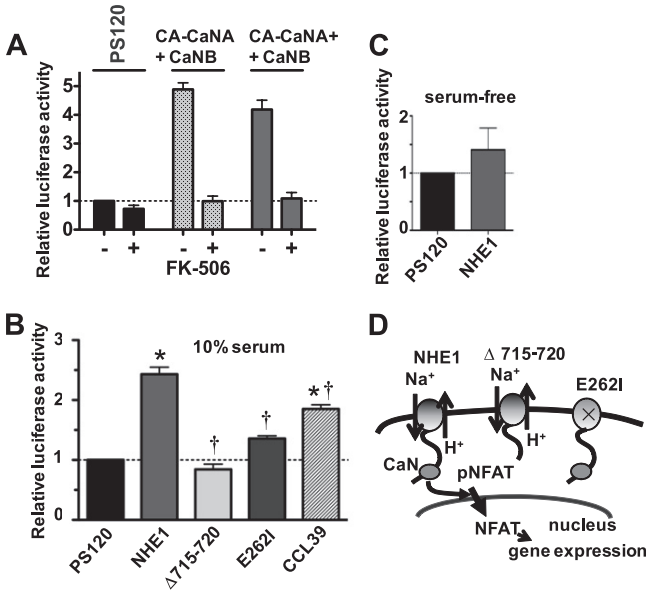


**FIG 3** Effect of the expression of NHE1 variants on NFAT promoter activity. (A) Effect of CA-CaNAα or CA-CaNAβ expression on NFAT-induced luciferase activity in the presence or absence of 1 μM FK506. The luciferase activity was normalized to that of the nontransfected control PS120 cells. Results ($n$ = 4) are shown as means ± SD. (B and C) Effects of the expression of wild-type and mutant NHE1 on NFAT promoter activity in the presence or absence of serum, respectively. PS120 cells that expressed each NHE1 variant or CCL39 cells expressing endogenous NHE1 were transfected with luciferase reporter plasmids and then incubated for 17 h in serum-depleted or supplemented growth media, respectively, and the luminescence was measured. The luciferase activity was normalized to that of nontransfected PS120 cells. Results ($n$ = 4) are shown as means ± SD. *, $P < 0.05$ versus nontransfected PS120 cells; †, $P < 0.05$ versus NHE1 wild type. (D) The diagram illustrates the properties of NHE1 mutants.

NHE1 activity potentiates serum-induced nuclear translocation of NFAT via activation of CaN. To quantify the results, cells were fixed under various conditions, and the nucleus/cytosol fluorescence ratio was analyzed and represented in histograms (Fig. 4C to E). These data indicate that (i) serum promoted nuclear translocation of NFAT, as evidenced by serum-induced increase in the median value in NHE1-transfectants (compare Fig. 4C to E), and (ii) the $Na^+/H^+$ exchange activity is required to potentiate the serum-induced nuclear translocation, because the median values were reduced by the presence of EIPA or the absence of NHE1 (untransfected PS120 cells) (Fig. 4D and E). To further verify the involvement of NHE1, we also examined the effect of EIPA on nuclear export of NFAT in cells that initially showed nuclear localization of NFAT in the presence of serum. FK506 induced nuclear export of NFAT in all 10 cells (Fig. 4F and G), indicating that NFAT export depends on termination of CaN signal. Treatment (1 h) with EIPA resulted in nuclear export of NFAT in 13 out of 19 cells (Fig. 4F and G). Such EIPA-induced nuclear export was also observed in CCL39 cells (7 out of 20 cells). These data suggest that inhibition of NHE1 activity resulted in a reduction of CaN signal in the subpopulation of cells with nuclear NFAT.

To determine whether CaN binding is required for NHE1-induced NFAT activation, we examined the effect of expression of the Δ715–720 NHE1 mutant (Fig. 5A) on the NFAT pathway. Similar to the wild-type NHE1, this deletion mutant retained high exchange activity (Fig. 5B) and was activated in response to extra-

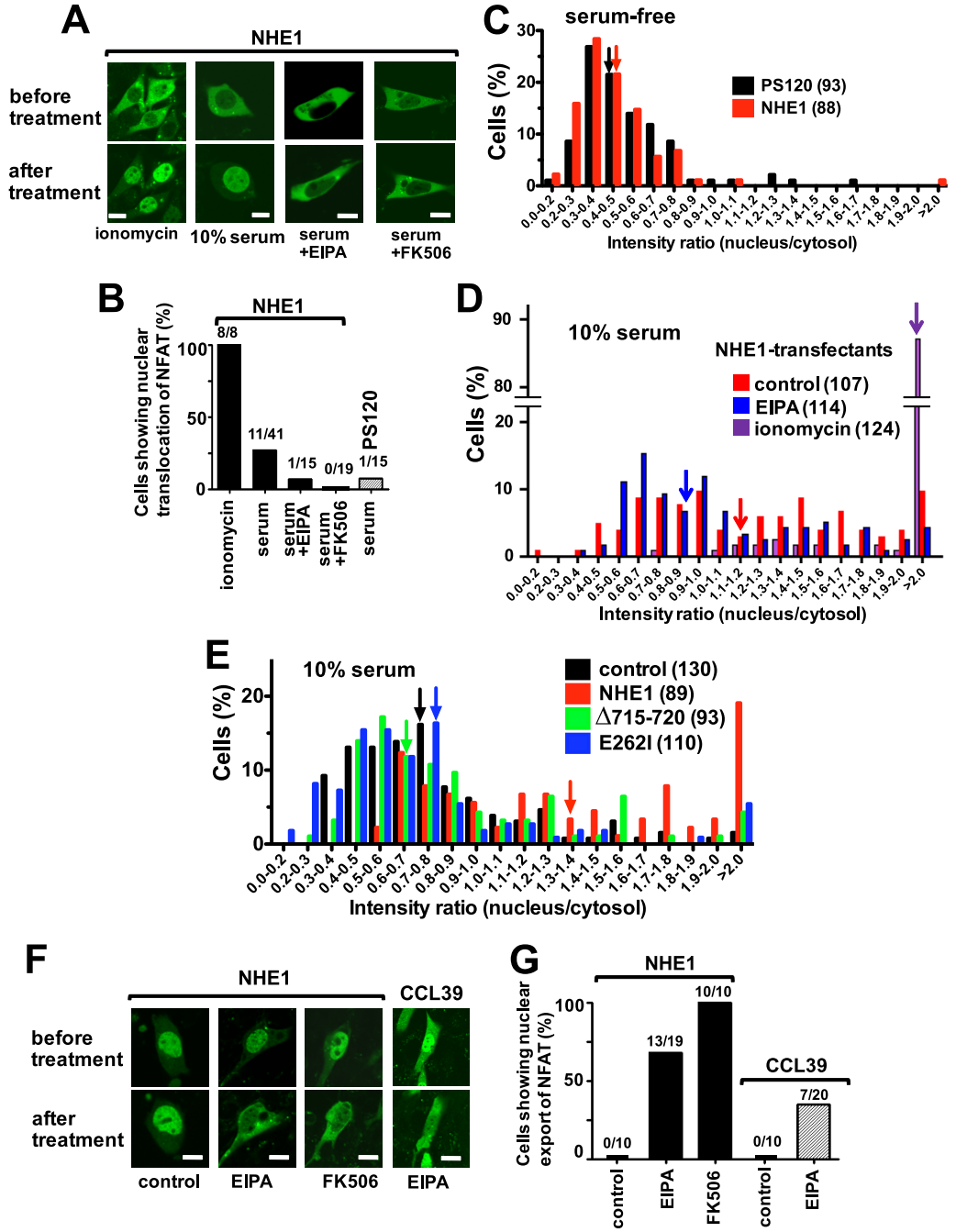


**FIG 4** Effect of NHE1 on nuclear translocation of NFAT. (A) Typical micrographs demonstrating subcellular localization of GFP-tagged NFAT. Cells expressing the wild-type NHE1 were transfected with hNFATc1-GFP and serum depleted. Cells showing extranuclear localization of NFAT (nucleus/cytosol fluorescence ratio of <1.0) were selected and then treated with 1 μM ionomycin or 10% serum in the presence or absence of 10 μM EIPA or 1 μM FK506. One hour later (15 min for ionomycin), localization of NFAT in the same cells as before treatment. Scale bar, 10 μm. (B) Percentage of cells showing nuclear translocation (fluorescence ratio of >1.0). The numbers indicate cells with a ratio of >1.0 among total selected cells. (C to E) The ratio of the GFP fluorescence intensity between the nucleus and cytosol is shown as a histogram. Cells were fixed, observed by confocal microscopy, and analyzed by imaging software. Arrows indicate the columns in which the medians are included, while numbers in parentheses show the number of cells analyzed. (C) Data for PS120 or NHE1 transfectants under serum-depleted conditions. (D) NHE1-transfected cells were treated for 1 h with EIPA or for 15 min with ionomycin in growth medium. (E) Data for control PS120 cells or transfectants of each NHE1 variant in growth medium. (F) In the presence of 10% serum, NHE1 transfectants or CCL39 cells showing nuclear localization of NFAT (ratio of >1.0) were selected and treated for 1 h with various agents. EIPA and FK506 promoted nuclear export of NFAT in many cells. The same cells were observed before and after treatment. Scale bar, 10 μm. (G) Percentage of cells showing nuclear export (fluorescence ratio of <1.0). The numbers indicate cells with a ratio of <1.0 among total selected cells.

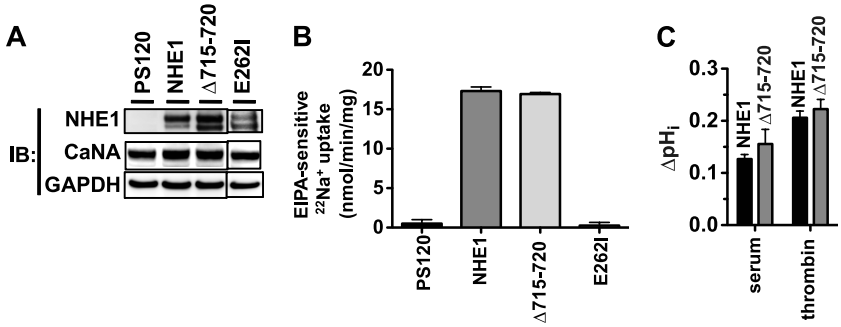


**FIG 5** Transport activity and regulation in response to stimuli in NHE1 variants. (A) Expression levels of NHE1, CaNA, and GAPDH (control). Expression of the wild-type NHE1 or NHE1 mutants did not affect the expression level of endogenous CaNA. (B) EIPA-sensitive $^{22}Na^+$-uptake activity (at $pH_i$ 5.4) in untransfected PS120 cells or cells expressing wild-type or mutant NHE1. Results ($n = 3$) are shown as means ± SD. (C) Change in $pH_i$ at 15 min after stimulation with 10% dialyzed fetal calf serum or 2 U · $ml^{-1}$ thrombin. The results ($n = 3$) are shown as means ± SD.

cellular stimuli (serum or thrombin), as shown by cytosolic alkalinization (Fig. 5C). However, the CaN-binding-deficient Δ715–720 NHE1 mutant was unable to induce transcriptional activation (Fig. 3B) and reduced the NHE1-induced nuclear translocation of NFAT (Fig. 4E), suggesting that the interaction between CaN and NHE1 is required for NHE1-induced activation of the CaN/NFAT pathway. Similarly, the E262I NHE1 mutant, possessing the CaN-binding site (Fig. 2A) but lacking $Na^+/H^+$ exchange activity (Fig. 5B), had little effect on NHE1-induced transcriptional activation (Fig. 3B) and nuclear translocation of NFAT (Fig. 4E), indicating that $Na^+/H^+$ exchange activity is also required for NHE1-induced activation of NFAT signaling (Fig. 3D).

**CaN activity is pH dependent.** Based on the above findings, we predicted that the $pH_i$ increase produced by NHE1 may be important for the further activation of CaN bound to NHE1 upon stimulation of cells with $Ca^{2+}$-mobilizing agonists. To test this hypothesis, we first examined whether CaN activity is pH dependent *in vitro*. In the presence of $Ca^{2+}$ (0.5 mM) and CaM (0.25 μM), CaN activity was greatly increased upon elevation of the pH from 6.3 to 8.6 and slightly decreased at more alkaline pH values (Fig. 6A). Interestingly, increasing the pH also increased the $Ca^{2+}$ sensitivity of CaN (Fig. 6B) by elevating its dissociation constant ($pK_d$) value for $Ca^{2+}$ and the Hill coefficient (Fig. 6C). Therefore, these findings indicate that CaN activity is modulated by both pH and [$Ca^{2+}$] in a mutually related fashion.

In order to examine whether binding to NHE1 itself is required to activate CaN, we measured the CaN activity in the presence or absence of NHE1-derived peptide. Inclusion of an excess amount of NHE1 peptide did not affect the CaN activity at various pH levels (Fig. 6D), suggesting that interaction with NHE1 by itself does not modulate the CaN activity. We also examined the effect of monovalent cations on CaN activity, as $Na^+/H^+$ exchange results in increased intracellular [$Na^+$], which may affect the activity of CaN. However, CaN activity was not influenced by the substitution of $Na^+$ with equimolar concentrations of other monovalent cations (e.g., $K^+$ or choline$^+$) (Fig. 6E). These results suggest that an increase in pH, but not in [$Na^+$], can activate CaN in cells at physiologically relevant $Ca^{2+}$ concentrations (0.1 to 1 μM).

Because CaN activity is pH dependent, we next addressed whether $pH_i$ affects the CaN/NFAT pathway. We examined the effect of extracellular pH ($pH_o$) on luciferase activity because an alkaline $pH_o$ stimulates $Na^+/H^+$ exchange activity and elevates the $pH_i$ (Fig. 6F) (28). Elevation of the $pH_o$ from 7.0 to 7.8 increased $pH_i$ and stimulated luciferase activity in cells that expressed wild-type NHE1, while the same treatment stimulated activity only slightly in cells expressing the Δ715-720 mutant; activation did not occur in untransfected PS120 cells or E262I transfectants (Fig. 6F). These results indicate that an increase in cytosolic pH can activate downstream CaN, especially when bound to NHE1.

**Effect of lipid rafts on NHE1-induced NFAT signaling.** The pH-dependent activation of CaN may occur in a restricted microdomain produced by NHE1 because CaN bound to NHE1 may be more activated by pH elevation driven by $Na^+/H^+$ exchange in the vicinity of clustered NHE1. Therefore, we addressed whether NHE1 exists in microdomains like lipid rafts, and if so, whether disruption of lipid rafts inhibits NHE1-induced NFAT activation. First, we examined the subcellular localization of CaN in the absence or presence of NHE1 expression. Endogenous CaN was diffusely localized in the cytosol and the plasma membrane (Fig. 7A). With expression of NHE1, a portion of CaN was clearly colocalized with NHE1 (Fig. 7A; see yellow color in cells), suggesting that these 2 proteins closely exist in the plasma membranes. Observation of the top of the cell surface by confocal microscopy revealed the presence of NHE1 as punctated spots (~200 nm) in the plasma membrane (Fig. 7B), although such spots of CaN were difficult to detect because of high background staining. Similarly, the lipid raft marker ganglioside GM1, which displayed the typical punctate staining pattern of lipid rafts, was partially (~50%) colocalized with NHE1. Furthermore, sucrose density gradient centrifugation revealed that a considerable amount of NHE1 was recovered in the detergent-resistant light fraction (fractions 4 and 5), in which another lipid raft marker (flotillin-1) cosedimented with NHE1 (Fig. 7C). These data suggest that a portion of NHE1 exists in lipid rafts. While over 90% of CaN was recovered in the nonraft heavy fraction, a small amount of CaN was also detected in the flotillin-1-rich light fraction. Treatment of cells with an agent that disrupts lipid rafts (MβCD) inhibited the colocalization of NHE1 with GM1 (Fig. 7B) and also reduced the amounts of NHE1, flotilin-1, and CaN in the light fraction (Fig. 7C). Under similar conditions, MβCD significantly reduced NHE1-induced transcriptional activity (Fig. 7D), although it did not affect the exchange activity itself, since the $^{22}Na^+$ uptake activities at $pH_i$ 5.4 were 19.8 ± 0.33 and 21.9 ± 0.21 nmol · $mg^{-1}$ · $min^{-1}$ [$n = 3$] for the control and MβCD treatment arm, respectively. These data

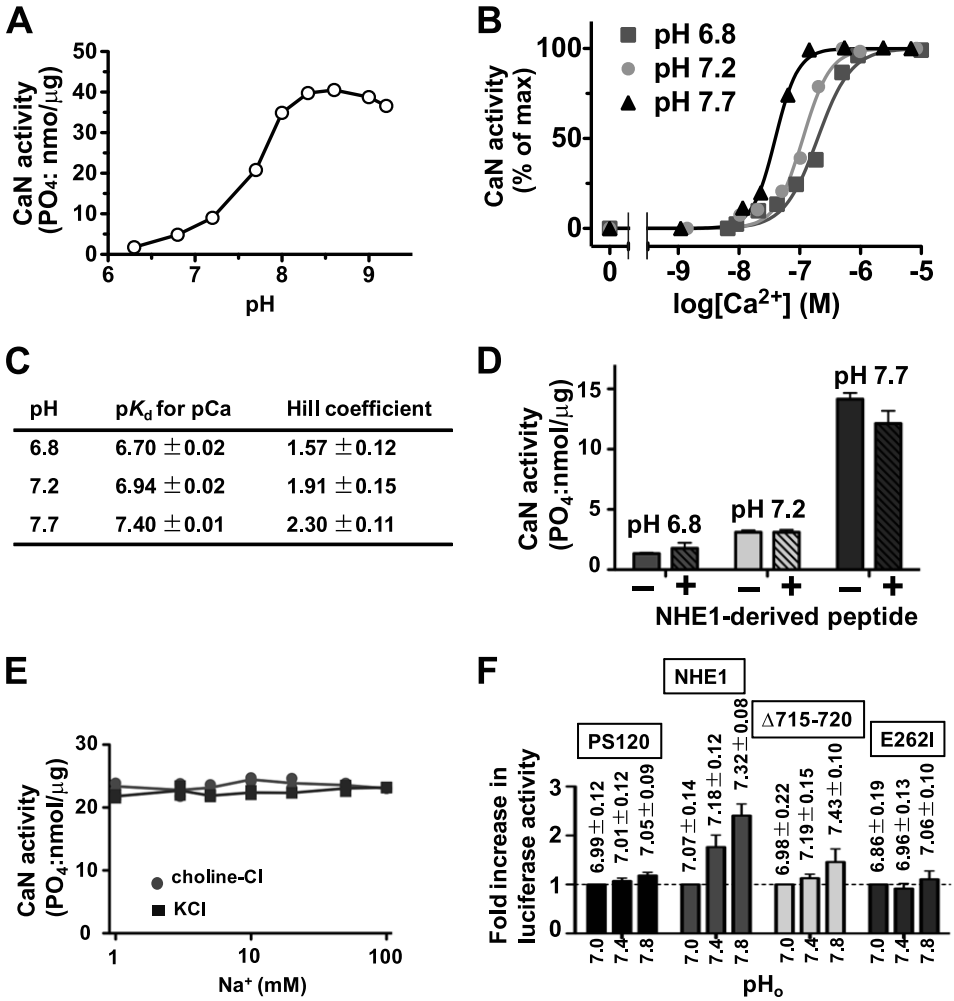


**FIG 6** CaN activity is pH dependent. (A) pH dependence of purified recombinant CaN activity (40 U CaN · well$^{-1}$) in the presence of 0.5 mM $CaCl_2$ and 0.25 μM CaM. (B) Effect of pH on the $Ca^{2+}$ dependence of CaN activity. The activity of CaN was measured under 3 different pH conditions in the presence of 0.1 mM $CaCl_2$ and 0.09 to 25 mM EGTA, which produced various concentrations of free $Ca^{2+}$. The data are expressed as the mean of 2 measurements. (C) p$K_d$ and Hill coefficient values obtained by fitting the curves shown in panel B. The best-fitting values ± the standard errors of the mean (SEM) are listed. (D) Effect of NHE1-derived peptide on CaN activity. CaN activity was measured at various pH values in the presence of $CaCl_2$/CaM and 5.6 μM CaN (40 U · well$^{-1}$), with or without 50 μM peptide containing the PVITID sequence. (E) Effect of monovalent cations on CaN activity. $Na^+$ present in the reaction medium was replaced by equimolar concentrations of choline$^+$ or $K^+$. (F) Dependence of extracellular pH ($pH_o$) on NFAT-induced luciferase activity. Cells that expressed wild-type or mutant NHE1 were incubated for 17 h in bicarbonate-free HEPES-buffered growth medium at the indicated pH values. The luciferase activity was normalized to that observed at pH 7.0. The results ($n = 4$) are expressed as means ± SD. Numbers indicate the $pH_i$ values measured at each $pH_o$ in HEPES-buffered bicarbonate-free solution by using the dual-excitation ratiometric pH indicator BCECF/AM. Data for $pH_i$ ($n \geq 10$) are represented as means ± SD.

suggest that the NHE1-induced amplification of CaN/NFAT signaling at least partly depends on NHE1 clustering in lipid rafts.

**CaN bound to NHE1 can dephosphorylate the nearby substrate.** An important question is how CaN bound to NHE1 promotes NFAT dephosphorylation in cells. Since we do not have the appropriate methodology to selectively measure the activity of the CaN bound to NHE1 in cells, we designed a model experiment using an NHE1-conjugated CaN substrate and examined whether this substrate is actually dephosphorylated by CaN. We constructed C-terminally truncated NHE1 (designed to optimize the distance between the CaN-binding site and RII tag) tagged with the CaN substrate peptide RIIpep and HA (designated NHE1*-RIIpep-HA) (Fig. 8A). NHE1*-RIIpep-HA was expressed in PS120 cells and immunostained with anti-HA and anti-phospho RII antibodies to detect the phosphorylation state of RII. In untransfected control cells, endogenous phosphorylated RII was mainly detected in the cytosol (Fig. 8B, upper panels), whereas phosphorylated RIIpep fused to NHE1 was mainly detected in the plasma membrane (Fig. 8B, lower panels). Interestingly, treatment with ionomycin resulted in significant dephosphorylation of RIIpep fused to NHE1 possessing a CaN-binding site, but not in the Δ715–720 NHE1 mutant (Fig. 8C and D). We examined the time courses of dephosphorylation of RIIpep after stimulation of cells with 2 $Ca^{2+}$-mobilizing agents, ionomycin and thrombin. Based on the previous findings, ionomycin and thrombin were expected to activate NHE1 (46) and CaN via $Ca^{2+}$ mobilization. These agents resulted in transient dephosphorylation of the RII tag, which was inhibited by FK506 (Fig. 8E and F). Thus, these

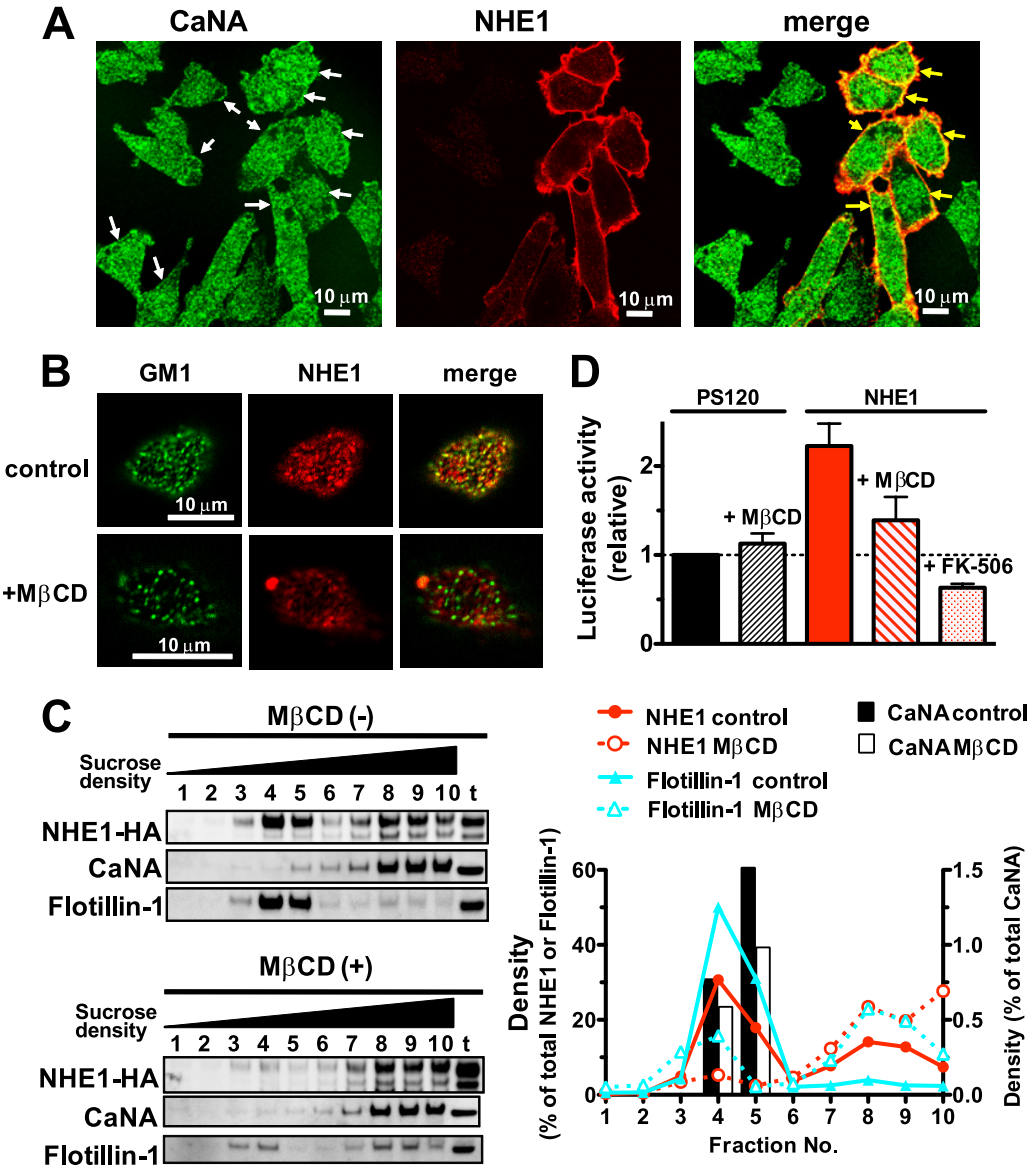


**FIG 7** NHE1-dependent activation of the NFAT pathway partially depends on the clustering of NHE1 in lipid rafts. (A) Subcellular localization of CaN in the absence or presence of expressed NHE1. NHE-deficient PS120 cells were transiently transfected with HA-tagged NHE1 (NHE1-2HA). Plasma membrane NHE1 was stained with anti-HA (extracellular tag, red) after fixation. Cells were permeabilized, and endogenous CaN was stained with rabbit anti-CaNA (green). CaN was diffusely localized throughout the cell. Note the plasma membrane localization of CaNA in both cells with and those without expressed NHE1 (white arrows) and partial colocalization of CaN and NHE1 (yellow regions in the merged photograph). (B) Subcellular localization pattern of NHE1 in the presence or absence of a lipid raft destabilizer, MβCD. Cells that expressed NHE1 were treated for 17 h with or without MβCD and fluorescently labeled for ganglioside GM1 (a lipid raft marker; green) and NHE1 (red). Cells were analyzed with a confocal microscope by adjusting the focal plane to near the top of the cells. In the absence of MβCD, NHE1 appeared as punctated spots that colocalized with GM1. (C) Immunoblotting (left column) of the fractions separated by sucrose density gradient centrifugation. Flotillin-1 was used as a lipid raft marker. The relative density of the protein bands was plotted (right panel). For CaNA, the protein densities in fractions 4 and 5 only were plotted. t, total lysate. (D) Effect of MβCD (3 mM) on the NHE1-induced stimulation of luciferase activity in PS120 or NHE1-transfected cells in the presence of serum-supplemented growth media. The effect of FK506 (1 μM) was also examined. Results ($n = 4$) are shown as means ± SD. *, $P < 0.05$ versus MβCD-free conditions.

findings suggest that $Ca^{2+}$ mobilization activates CaN bound to NHE1, which results in dephosphorylation of nearby substrates.

**NHE1 promotes hypertrophic signaling in cardiomyocytes, partly through binding to CaN.** In order to examine the pathological relevance of the NHE1-CaN interaction, we addressed whether CaN binding plays a role in NHE1-induced activation of hypertrophic signaling in neonatal rat ventricular myocytes. Overexpression of HA-tagged NHE1 (NHE1-2HA) significantly promoted the nuclear translocation of NFAT (Fig. 9A and B). However, NFAT translocation induced by the Δ715–720 NHE1 mutant was less efficient than that of wild-type NHE1. FK506 inhibited NHE1-induced translocation of NFAT (Fig. 9B). These data demonstrate that CaN binding is involved in NHE1-dependent nuclear translocation of NFAT in cardiomyocytes.

Adenovirus expression of NHE1-2HA in cardiomyocytes (Fig. 10A and B) resulted in significant upregulation of a hypertrophic

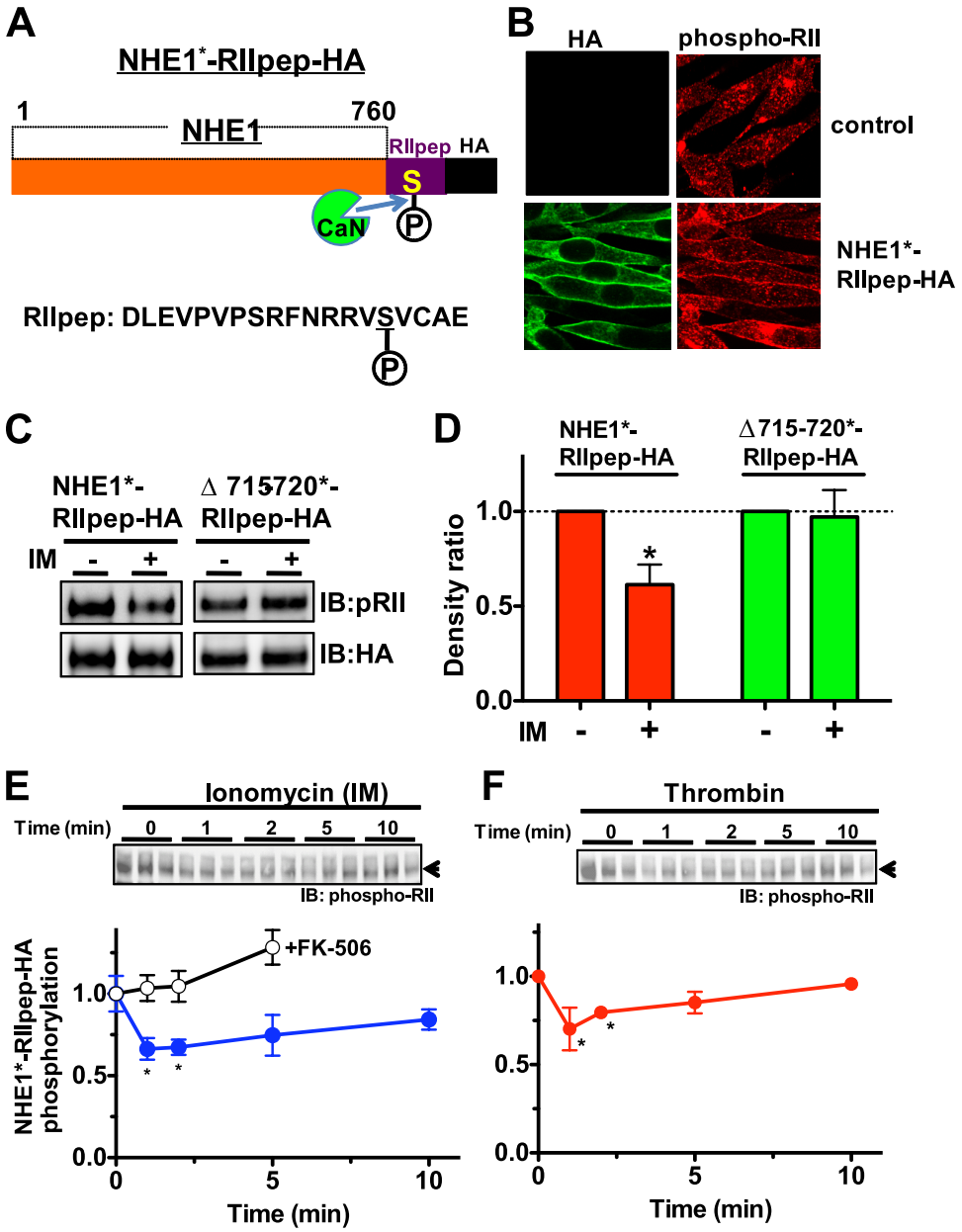


**FIG 8** CaN substrate conjugated to NHE1 is dephosphorylated in response to $Ca^{2+}$-mobilizing reagents. (A) Schematic representation of truncated NHE1 tagged with RIIpep and HA (designated NHE1*-RIIpep-HA). (B) Immunostaining with anti-phospho RII antibody for detection of phosphorylation of NHE1-conjugated RIIpep or endogenous RII and with anti-HA for detection of NHE1. NHE1*-RIIpep-HA was expressed in PS120 cells (bottom panels). (C) Immunoblot showing the effect of ionomycin (IM) on the phosphorylation state of RIIpep tagged to NHE1. Two minutes after stimulation with IM (3 μM) under serum-free conditions, the reaction was terminated by replacing the medium with PAGE sample buffer, and immunoblotted with anti-phosphoRII (pRII) or anti-HA antibodies. (D) Summarized data obtained from the immunoblot shown in panel C. The density of the pRII band was normalized to that of HA in the same sample. Results ($n = 4$) are expressed as means ± SD. IM induced significant dephosphorylation of RIIpep-tag in cells expressing NHE1*-RIIpep-HA but not in cells expressing the CaN-free NHE1 mutant, suggesting that CaN bound to NHE1 can dephosphorylate nearby substrates. *, $P < 0.05$, unpaired Student's *t* test versus control. (E and F) Time course of the change in the phosphorylation level of RIIpep tagged to NHE1 in response to IM (3 μM) or thrombin ($2\ U \cdot ml^{-1}$), respectively. The lysates were subjected to PAGE and then immunoblotted with an anti-pRII antibody. Results ($n = 3$) are shown as means ± SD. In one experiment, the CaN-inhibitor FK506 (1 μM) was added simultaneously to the cells with IM.

marker protein, atrial natriuretic factor (ANF), as shown by immunoblot analysis (Fig. 10A and C). Overexpression of NHE1-2HA also produced an increase in the number of myocytes expressing ANF, which was observed by intense perinuclear immunostaining (Fig. 10D and E). In addition, overexpression of NHE1-2HA resulted in an increase in the expression of CaN-dependent hypertrophic marker RCAN1 (Fig. 10F and G). Furthermore, overexpression of NHE1-2HA resulted in enlargement of cardiomyocyte size (Fig. 10H). Thus, NHE1 stimulated hypertrophic signal transduction in cardiomyocytes, albeit to a lesser extent than treatment with a known hypertrophic stimulant, phenylephrine (PE), as a positive control. The NHE1 Δ715–720

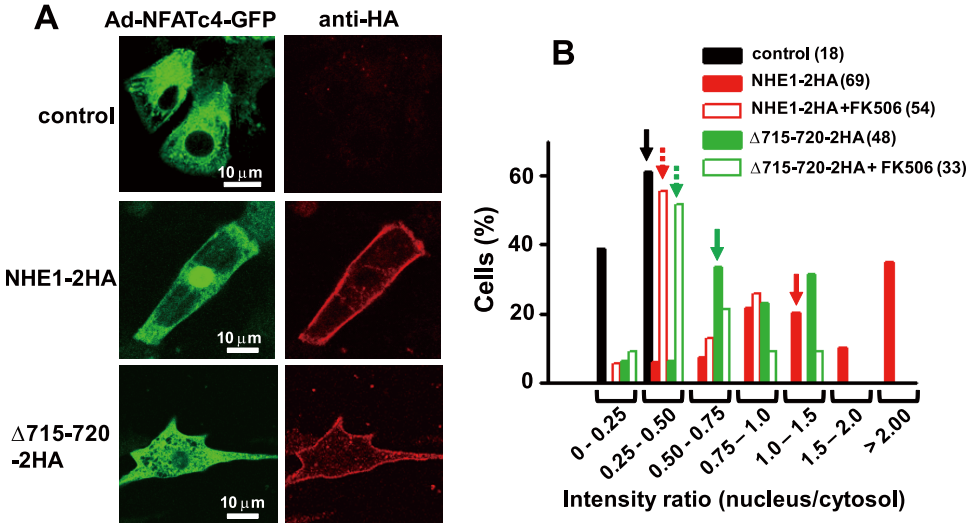


**FIG 9** Overexpression of NHE1 induces nuclear translocation of NFAT in cardiomyocytes. (A) Typical micrographs showing the subcellular localization pattern of NFAT in neonatal rat ventricular myocytes under serum-free conditions with or without expression of NHE1 variants. Cardiomyocytes were transfected with plasmids carrying the extracellular HA-tagged wild-type NHE1 or Δ715–720 mutant NHE1, followed by infection with adenovirus carrying NFATc4-GFP. Cells were subsequently fixed and immunostained with anti-HA antibody to detect the sarcolemmal expression of NHE1. (B) The ratio of GFP fluorescence intensity between the nucleus and cytosol is shown as a histogram. Arrows indicate the columns in which the medians are included, while the numbers in parentheses show the number of cells analyzed.

mutant, however, was much less efficient than the wild-type NHE1 at activating hypertrophic signaling (Fig. 10A to H). FK506 inhibited NHE1-induced hypertrophic signaling. Thus, the CaN-NHE1 interaction is important for activation of the downstream NFAT pathway, serving as a major route for NHE1-induced hypertrophic responses in cardiomyocytes.

## DISCUSSION

In the present study, we demonstrated that the CaNA subunit directly binds to the cytoplasmic domain of NHE1 via the latter's PVITID sequence. Expression of NHE1 in fibroblasts further promoted serum-induced nuclear translocation of NFAT and enhanced gene transcription driven by the NFAT response element. Subcellular localization of NFAT depends on the balance between phosphorylation and CaN-dependent dephosphorylation (19). The NHE1 inhibitor EIPA inhibited serum-induced nuclear import of NFAT and potentiated nuclear export of NFAT, suggesting a link between $Na^+/H^+$ exchange activity and the CaN/NFAT pathway. In neonatal rat ventricular myocytes, overexpression of NHE1 activated hypertrophic gene expression and stimulated the nuclear translocation of NFAT—responses that were inhibited by a CaN inhibitor, FK506. Thus, we propose that NHE1 functions as a positive regulator of the CaN-mediated signaling pathway, leading to cardiomyocyte hypertrophy.

We demonstrated that both CaN binding and $Na^+/H^+$ exchange activity are required for NHE1-induced amplification of NFAT signaling. Since NHE1 mediates a powerful $H^+$-extrusion pathway across the plasma membrane, we hypothesized that under $Ca^{2+}$ mobilization, CaN is further activated by its recruitment to a high-pH microenvironment, which is produced by clustered NHE1 (Fig. 11A). Indeed, CaN activity was highly pH dependent and was stimulated as the pH increased in the physiological range from 7.0 to 8.0 in the presence of $Ca^{2+}$-CaM complex (Fig. 6A). However, the optimal pH of CaN activity measured in our study (pH 8.5) differs from those reported in earlier studies (~ pH 7.0) (39, 52), which is likely to result from the different experimental conditions employed. CaN activator CaM contains 4 EF-hand motifs that each bind to $Ca^{2+}$. Therefore, the highly cooperative activation of CaN by $Ca^{2+}$ (Fig. 6B) is partly due to the cooperative binding of $Ca^{2+}$ to the 4 EF-hand domains of CaM (8, 13, 25). CaN is also activated in response to increasing pH, which increases the affinity of CaN for $Ca^{2+}$ (Fig. 6B) and the Hill coefficient for $Ca^{2+}$ activation (Fig. 6C). These data suggest that augmentation of the pH activates CaN, even at low intracellular $Ca^{2+}$ concentrations (~$10^{-7}$ M). Thus, NHE1-mediated activation of CaN may occur via increased binding of $Ca^{2+}$ to CaM and accelerated catalytic activity of the CaNA subunit at high pH.

The strong pH sensitivity of CaN raises the interesting possibility that NHE1 provides a spatially restricted platform for CaN activation by producing a high-pH microenvironment. Indeed, using an NHE1-bound pH probe that we recently designed, we obtained evidence that NHE1 can produce a high local pH in the vicinity of NHE1 (unpublished data). NHE1 accumulated in restricted patches (~200 nm) in the plasma membrane, observed by confocal microscopy. We observed colocalization of NHE1 with GM1 and cosedimentation of NHE1 with flotillin-1, suggesting that a substantial portion of NHE1 is localized in lipid rafts, consistent with earlier studies (5, 55). Lipid rafts are dynamic assemblies enriched in sphingolipid, cholesterol, and glycosylphosphatidylinositol (GPI)-anchored proteins, and clustered lipid rafts may serve as heterogeneous platforms that facilitate efficient signaling (32). Interestingly, disruption of lipid rafts with MβCD markedly inhibited NHE1-induced NFAT promoter activity, suggesting that accumulation of NHE1 in lipid rafts is at least partly required for NHE1-induced CaN/NFAT signal amplification.

Cellular endogenous CaN was diffusely distributed in fibroblasts (Fig. 7A) and in cardiomyocytes (data not shown). Partial localization of CaN in plasma membranes suggests that some CaN is targeted to multiple membranes or membrane-anchored pro-

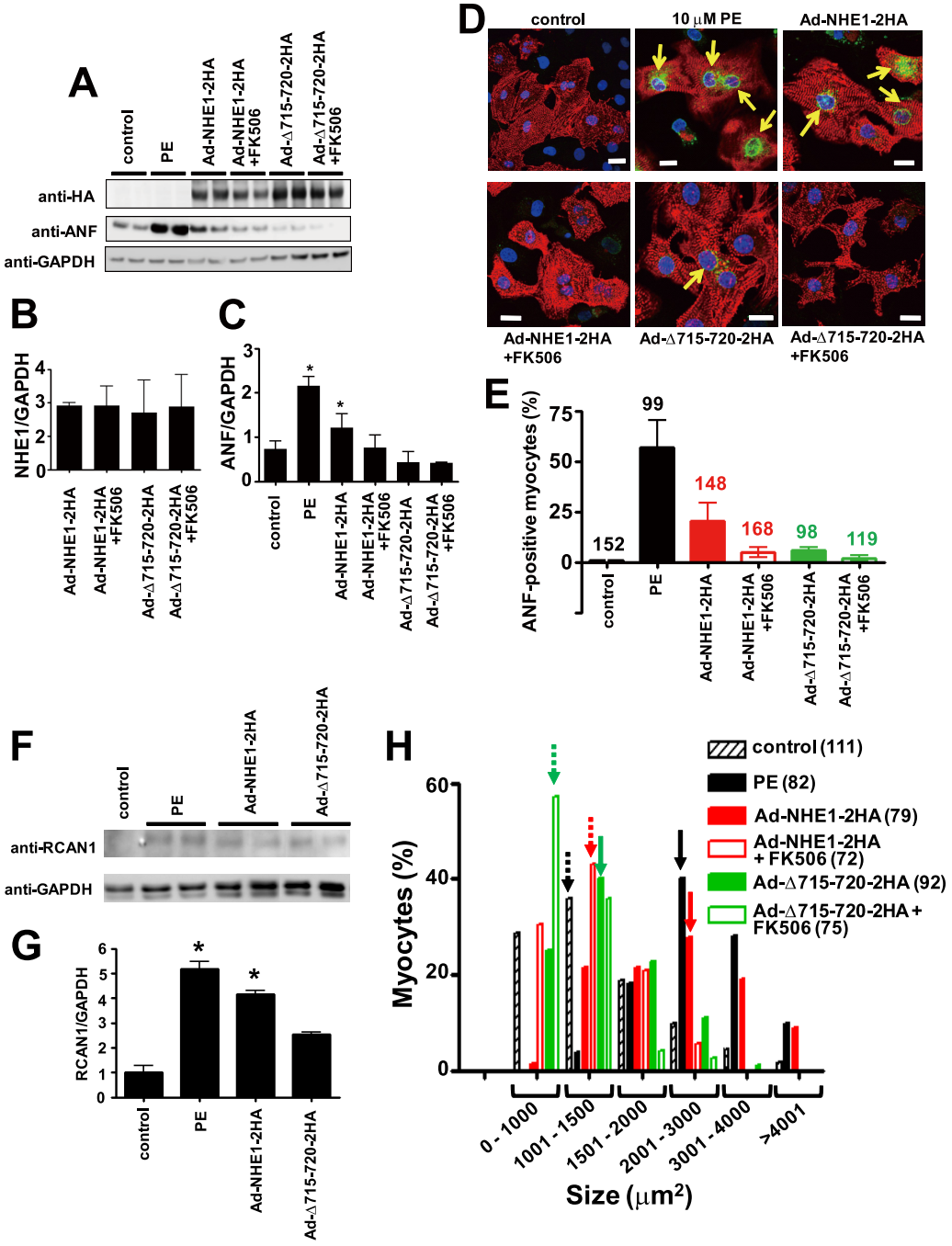


**FIG 10** CaN-binding is required for NHE1-induced cardiomyocyte hypertrophy. (A, B, and C) The hypertrophic marker ANF is upregulated by overexpression of wild-type NHE1, but not by a CaN-free NHE1 mutant. Cardiomyocytes were infected with adenovirus carrying HA-tagged wild-type NHE1 or the Δ715–720 mutant and then treated with or without FK506 (1 μM). As a control experiment, myocytes were treated with 10 μM phenylephrine (PE). The expression levels of HA-tagged NHE1 and ANF were examined by immunoblotting and are represented as a ratio of GAPDH (internal control). Results ($n = 4$) are shown as means ± SD. *, $P < 0.05$ versus control. (D) The expression level of ANF in cardiomyocytes was analyzed by immunofluorescence. Myocytes were treated as indicated and subsequently immunostained with anti-ANF (green) and anti-α-actinin (cardiomyocyte marker; red) antibodies. Nuclei were labeled with DAPI (blue). In some cells (arrows), strong staining of ANF around the nucleus was detected. (E) The expression of ANF was analyzed in >3 different microscopic fields. Results are shown as means ± SD, and the number of myocytes analyzed is indicated. (F and G) Expression of CaN-dependent hypertrophic marker RCAN1 in cardiomyocytes treated as described above (A). (H) Histogram showing the effect of several treatments on cardiomyocyte size. Myocytes were treated as indicated and immunostained with anti-α-actinin antibody for the detection of myocytes, followed by DAPI staining for the detection of nuclei. The area of myocytes ($\mu m^2$) was measured by an FV1000 confocal microscope (Olympus) equipped with imaging software. The expression of NHE1 or treatment with 10 μM PE resulted in the enlargement of a greater number of myocytes than that observed for expression of the Δ715–720 deletion mutant. FK506 (1 μM) inhibited NHE1-induced myocyte hypertrophy. Arrows show columns in which the medians are included.

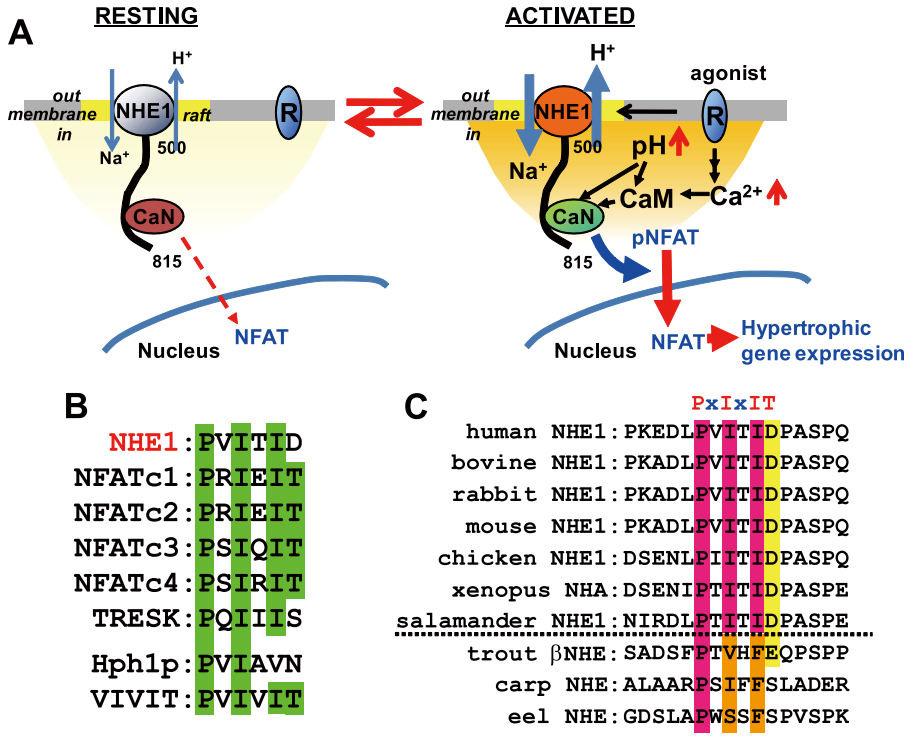


**FIG 11** Schematic representation of the NHE1-dependent activation of the CaN/NFAT pathway and alignment of the PXIXIT motif. (A) Possible mechanism for the NHE1-dependent activation of CaN/NFAT signaling. In the resting state (left), NHE1 may moderately activate the CaN/NFAT pathway. In the activated state (right), activation of NHE1 in response to serum or receptor agonists increases $pH_i$ in the vicinity of NHE1 and further amplifies the CaN/NFAT pathway under $Ca^{2+}$ mobilization. (B) Conservation of the PXIXIT motif within several CaN-binding proteins. Amino acid sequence alignment of the CaN-binding motifs of NHE1, human NFAT, human TWIK-related spinal cord $K^+$ channel (TRESK) (9), *Saccharomyces cerevisiae* Hph1 (14), and a high-affinity CaN-binding peptide (PVIVIT) (2). GenBank accession numbers are as follows: NFATc1, NP_765978; NFATc2, NP_001129493; NFATc3, NP_775188; NFATc4, NP_001129494; TRESK, NP_862823; and Hph1, NP_014969. (C) Alignment of the PXIXIT sequence among NHEs from different animals. The PXIXIT-like motif is conserved in NHE1 from amphibians to mammals, but not in fish, and is not found in mammalian NHE2, NHE3, NHE4, or NHE5.

teins. Our present study indicated that NHE1 is one of several membrane targets for CaN. The basal NFAT promoter activity in NHE1-deficient PS120 cells was inhibited slightly (20%) by FK506 (Fig. 3A). Furthermore, in most of the PS120 cells, NFAT was localized in the cytosol even after addition of serum (Fig. 4B, C, And E). Therefore, a large fraction of CaN does not appear to exist in the active form under serum-free or serum-supplemental culture medium in PS120 cells. Activation of the CaN/NFAT pathway by NHE1 suggests that NHE1 can sensitize CaN to activation in the plasma membrane. Activation or inhibition of CaN/NFAT signaling has been suggested to occur in plasma membrane microdomains due to changes in the local $Ca^{2+}$ concentration, which are caused by $Ca^{2+}$-transport proteins—e.g., channels and pumps (4, 11, 16, 45). These studies support the hypothesis that CaN is efficiently regulated at more restricted membrane regions rather than in the cytoplasmic bulk space.

How is CaN binding required for NHE1-dependent NFAT activation? We hypothesize a possible role for NHE1 as a spatial and transient platform for CaN activation. $Ca^{2+}$-mobilizing stimuli activate NHE1 and result in elevation of $pH_i$, particularly at the submembranous region close to clustered NHE1 (Fig. 11A). We observed that interaction with NHE1 itself does not affect the CaN activity, which was similarly enhanced by increasing pH (Fig. 6D). Indeed, a model experiment suggested that CaN bound to NHE1 can be activated in response to stimulation in cells (Fig. 8). Therefore, external stimuli would lead to more efficient activation of CaN bound to NHE1 compared to bulk CaN through a pH-dependent increase in the catalytic activity and $Ca^{2+}$ sensitivity of CaN (Fig. 6A to C). In addition, CaM, which directly binds to NHE1 (3), may also contribute to activation of CaN bound in close proximity to NHE1. We showed that CaN is released from NHE1 by competitive peptides (Fig. 2B). Thus, activated CaN could be released from NHE1 by the competitive binding of other CaN-binding proteins, such as NFAT, with higher affinity to CaN. Furthermore, this process may be accelerated by an increase in pH (Fig. 2F). After binding to nearby NFAT, CaN would dephosphorylate NFAT, leading to downstream signaling (Fig. 11A). Additional studies will be required to ascertain such a hypothesis.

The CaN-binding site is located within the distal cytoplasmic region of NHE1 (aa 698 to 815), which has little effect on the basal exchange activity or its activation by intracellular $H^+$ and various extracellular stimuli (20, 47). Therefore, this distal region may function as a platform to transmit the ionic signals produced by NHE1 to downstream pH-sensitive enzymes. Adenylyl cyclase (51) also represents a possible downstream target of NHE1. The PXIXIT-like motif, which is only present in the ubiquitously expressed NHE1 isoform (Fig. 11B), is conserved in species from amphibians to mammals, but not in fish (Fig. 11C), suggesting the importance of the NHE1-CaN interaction in many tissues. The low homology in the distal C-terminal regions of NHE1 to -5 suggests a role in tissue-specific signal transduction from each NHE isoform to downstream targets bound to this region.

Pathological cardiac hypertrophy is an adaptive response that is partly triggered by the CaN/NFAT pathway (15). Recently, we demonstrated that transgenic expression of an activated form of NHE1 causes cardiac hypertrophy and heart failure due to activation of $Ca^{2+}$-dependent prohypertrophic factors (e.g., CaN and $Ca^{2+}$/CaM-dependent protein kinase II) via increased cytosolic [$Ca^{2+}$] and [$Na^{+}$] (37). Indeed, there are many reports demonstrating that the expression level of NHE1 is elevated in various hypertrophic animal models (12, 23, 24). In the present study, we demonstrated that overexpression of NHE1 resulted in cardiomyocyte enlargement and augmented hypertrophic gene (ANF and RCAN1) expression. This NHE1-mediated hypertrophic response is, at least in part, mediated by activation of the CaN/NFAT pathway, since (i) overexpression of a CaN-free NHE1 mutant produced only a small effect and (ii) NHE1-promoted nuclear translocation of NFAT, ANF expression, and cardiomyocyte hypertrophy were all inhibited by FK506. These findings imply that pH signals from NHE1 act synergistically with $Ca^{2+}$ signals to promote the progression of cardiomyocyte hypertrophy via amplification of the CaN/NFAT pathway. In this study, we did not analyze whether the NHE1/CaN/NFAT pathway is also involved in hormone-induced cardiac hypertrophy. However, NHE1 has been reported to be involved in this process. For example, the NHE1 inhibitor cariporide prevented β-adrenergic receptor-mediated cardiac hypertrophy, where NHE1 is upregulated (12). Therefore, NHE1-CaN signal relay may also be a possible pathway leading to hormone-induced cardiac hypertrophy. To our knowledge, this is the first report to describe activation of the CaN/NFAT signaling pathway by a pH-regulating membrane transporter.

## ACKNOWLEDGMENTS

This work was supported by Grants-in-Aid for Scientific Research on Priority Areas (no. 18077015 and 18059035), Grants-in-Aid for Scientific Research B (no. 19390080) and C (no. 23590105) and Exploratory Research (no. 22659046) from the Ministry of Education, Culture, Sports, Science and Technology, a grant for the Promotion of Fundamental Studies in Health Sciences from the National Institute of Biomedical Innovation (NIBIO), research grants for Cardiovascular Diseases (no. 20C-3 and 21A-13), and a grant from the Salt Science Research Foundation (no. 0836).

We thank Soushi Kobayashi, Hironori Hanada, Michitaka Masuda, Hitomi Ohtake, and Miho Miyazaki (National Cerebral and Cardiovascular Center Research Institute, Japan) for technical assistance.

## REFERENCES

1. **Ammar YB, Takeda S, Hisamitsu T, Mori H, Wakabayashi S.** 2006. Crystal structure of CHP2 complexed with NHE1-cytosolic region and an implication for pH regulation. EMBO J. **25**:2315–2325.
2. **Aramburu J, et al.** 1998. Selective inhibition of NFAT activation by a peptide spanning the calcineurin targeting site of NFAT. Mol. Cell **1**:627–637.
3. **Bertrand B, Wakabayashi S, Ikeda T, Pouyssegur J, Shigekawa M.** 1994. The $Na^{+}/H^{+}$ exchanger isoform 1 (NHE1) is a novel member of the calmodulin-binding proteins. Identification and characterization of calmodulin-binding sites. J. Biol. Chem. **269**:13703–13709.
4. **Buch MH, et al.** 2005. The sarcolemmal calcium pump inhibits the calcineurin/nuclear factor of activated T-cell pathway via interaction with the calcineurin A catalytic subunit. J. Biol. Chem. **280**:29479–29487.
5. **Bullis BL, Li X, Singh DN, Berthiaume LG, Fliegel L.** 2002. Properties of the $Na^{+}/H^{+}$ exchanger protein. Detergent-resistant aggregation and membrane microdistribution. Eur. J. Biochem. **269**:4887–4895.
6. **Cardone RA, Casavola V, Reshkin SJ.** 2005. The role of disturbed pH dynamics and the $Na^{+}/H^{+}$ exchanger in metastasis. Nat. Rev. Cancer **5**:786–795.
7. **Crabtree GR.** 2001. Calcium, calcineurin, and the control of transcription. J. Biol. Chem. **276**:2313–2316.
8. **Crouch TH, Klee CB.** 1980. Positive cooperative binding of calcium to bovine brain calmodulin. Biochemistry **19**:3692–3698.
9. **Czirjak G, Enyedi P.** 2006. Targeting of calcineurin to an NFAT-like docking site is required for the calcium-dependent activation of the background $K^{+}$ channel, TRESK. J. Biol. Chem. **281**:14677–14682.
10. **Darmellah A, et al.** 2007. Enhanced activity of the myocardial $Na^{+}/H^{+}$ exchanger contributes to left ventricular hypertrophy in the Goto-Kakizaki rat model of type 2 diabetes: critical role of Akt. Diabetologia **50**:1335–1344.
11. **Eder P, Molkentin JD.** 2011. TRPC channels as effectors of cardiac hypertrophy. Circ. Res. **108**:265–272.
12. **Engelhardt S, Hein L, Keller U, Klambt K, Lohse MJ.** 2002. Inhibition of $Na^{+}$-$H^{+}$ exchange prevents hypertrophy, fibrosis, and heart failure in beta(1)-adrenergic receptor transgenic mice. Circ. Res. **90**:814–819.
13. **Gifford JL, Walsh MP, Vogel HJ.** 2007. Structures and metal-ion-binding properties of the $Ca^{2+}$-binding helix-loop-helix EF-hand motifs. Biochem. J. **405**:199–221.
14. **Heath VL, Shaw SL, Roy S, Cyert MS.** 2004. Hph1p and Hph2p, novel components of calcineurin-mediated stress responses in Saccharomyces cerevisiae. Eukaryot. Cell **3**:695–704.
15. **Heineke J, Molkentin JD.** 2006. Regulation of cardiac hypertrophy by intracellular signalling pathways. Nat. Rev. Mol. Cell Biol. **7**:589–600.
16. **Heineke J, Ritter O.** 2012. Cardiomyocyte calcineurin signaling in subcellular domains: from the sarcolemma to the nucleus and beyond. J. Mol. Cell. Cardiol. **52**:62–73.
17. **Hisamitsu T, Ben Ammar Y, Nakamura TY, Wakabayashi S.** 2006. Dimerization is crucial for the function of the $Na^{+}/H^{+}$ exchanger NHE1. Biochemistry **45**:13346–13355.
18. **Hisamitsu T, Pang T, Shigekawa M, Wakabayashi S.** 2004. Dimeric interaction between the cytoplasmic domains of the $Na^{+}/H^{+}$ exchanger NHE1 revealed by symmetrical intermolecular cross-linking and selective co-immunoprecipitation. Biochemistry **43**:11135–11143.
19. **Hogan PG, Chen L, Nardone J, Rao A.** 2003. Transcriptional regulation by calcium, calcineurin, and NFAT. Genes Dev. **17**:2205–2232.
20. **Ikeda T, Schmitt B, Pouyssegur J, Wakabayashi S, Shigekawa M.** 1997. Identification of cytoplasmic subdomains that control pH-sensing of the $Na^{+}/H^{+}$ exchanger (NHE1): pH-maintenance, ATP-sensitive, and flexible loop domains. J. Biochem. **121**:295–303.
21. **Karmazyn M, Gan XT, Humphreys RA, Yoshida H, Kusumoto K.** 1999. The myocardial $Na^{+}$-$H^{+}$ exchange: structure, regulation, and its role in heart disease. Circ. Res. **85**:777–786.
22. **Karmazyn M, Kilic A, Javadov S.** 2008. The role of NHE-1 in myocardial hypertrophy and remodelling. J. Mol. Cell. Cardiol. **44**:647–653.
23. **Karmazyn M, Sawyer M, Fliegel L.** 2005. The $Na^{+}/H^{+}$ exchanger: a target for cardiac therapeutic intervention. Curr. Drug Targets Cardiovasc. Haematol. Disord. **5**:323–335.
24. **Kilic A, et al.** 2005. Enhanced activity of the myocardial $Na^{+}/H^{+}$ exchanger NHE-1 contributes to cardiac remodeling in atrial natriuretic peptide receptor-deficient mice. Circulation **112**:2307–2317.
25. **Kincaid RL, Vaughan M.** 1986. Direct comparison of $Ca^{2+}$ requirements for calmodulin interaction with and activation of protein phosphatase. Proc. Natl. Acad. Sci. U. S. A. **83**:1193–1197.
26. **Klee CB, Draetta GF, Hubbard MJ.** 1988. Calcineurin. Adv. Enzymol. Relat. Areas Mol. Biol. **61**:149–200.
27. **Klee CB, Ren H, Wang X.** 1998. Regulation of the calmodulin-stimulated protein phosphatase, calcineurin. J. Biol. Chem. **273**:13367–13370.
28. **L'Allemain G, Paris S, Pouyssegur J.** 1984. Growth factor action and intracellular pH regulation in fibroblasts. Evidence for a major role of the $Na^{+}/H^{+}$ antiport. J. Biol. Chem. **259**:5809–5815.
29. **Lehoux S, Abe J, Florian JA, Berk BC.** 2001. 14-3-3 binding to $Na^{+}/H^{+}$ exchanger isoform-1 is associated with serum-dependent activation of $Na^{+}/H^{+}$ exchange. J. Biol. Chem. **276**:15794–15800.
30. **Li H, Zhang L, Rao A, Harrison SC, Hogan PG.** 2007. Structure of calcineurin in complex with PVIVIT peptide: portrait of a low-affinity signalling interaction. J. Mol. Biol. **369**:1296–1306.
31. **Lin X, Barber DL.** 1996. A calcineurin homologous protein inhibits GTPase-stimulated Na-H exchange. Proc. Natl. Acad. Sci. U. S. A. **93**:12631–12636.
32. **Lingwood D, Simons K.** 2010. Lipid rafts as a membrane-organizing principle. Science **327**:46–50.

33. **Mancini M, Toker A.** 2009. NFAT proteins: emerging roles in cancer progression. Nat. Rev. Cancer **9**:810–820.
34. **Matsushita M, et al.** 2007. Loss of calcineurin homologous protein-1 in chicken B lymphoma DT40 cells destabilizes $Na^+/H^+$ exchanger isoform-1 protein. Am. J. Physiol. Cell Physiol. **293**:C246–C254. doi: 10.1152/ajpcell.00464.2006.
35. **Molkentin JD, et al.** 1998. A calcineurin-dependent transcriptional pathway for cardiac hypertrophy. Cell **93**:215–228.
36. **Moncoq K, Kemp G, Li X, Fliegel L, Young HS.** 2008. Dimeric structure of human $Na^+/H^+$ exchanger isoform 1 overproduced in Saccharomyces cerevisiae. J. Biol. Chem. **283**:4145–4154.
37. **Nakamura TY, Iwata Y, Arai Y, Komamura K, Wakabayashi S.** 2008. Activation of $Na^+/H^+$ exchanger 1 is sufficient to generate $Ca^{2+}$ signals that induce cardiac hypertrophy and heart failure. Circ. Res. **103**:891–899.
38. **Orlowski J, Grinstein S.** 2004. Diversity of the mammalian sodium/proton exchanger SLC9 gene family. Pflugers Arch. **447**:549–565.
39. **Pallen CJ, Wang JH.** 1983. Calmodulin-stimulated dephosphorylation of p-nitrophenyl phosphate and free phosphotyrosine by calcineurin. J. Biol. Chem. **258**:8550–8553.
40. **Pouyssegur J, Sardet C, Franchi A, L'Allemain G, Paris S.** 1984. A specific mutation abolishing $Na^+/H^+$ antiport activity in hamster fibroblasts precludes growth at neutral and acidic pH. Proc. Natl. Acad. Sci. U. S. A. **81**:4833–4837.
41. **Roy J, Li H, Hogan PG, Cyert MS.** 2007. A conserved docking site modulates substrate affinity for calcineurin, signaling output, and in vivo function. Mol. Cell **25**:889–901.
42. **Rusnak F, Mertz P.** 2000. Calcineurin: form and function. Physiol. Rev. **80**:1483–1521.
43. **Sardet C, Franchi A, Pouyssegur J.** 1989. Molecular cloning, primary structure, and expression of the human growth factor-activatable $Na^+/H^+$ antiporter. Cell **56**:271–280.
44. **Slepkov ER, Rainey JK, Sykes BD, Fliegel L.** 2007. Structural and functional analysis of the $Na^+/H^+$ exchanger. Biochem. J. **401**:623–633.
45. **Tandan S, et al.** 2009. Physical and functional interaction between calcineurin and the cardiac L-type $Ca^{2+}$ channel. Circ. Res. **105**:51–60.
46. **Wakabayashi S, Bertrand B, Ikeda T, Pouyssegur J, Shigekawa M.** 1994. Mutation of calmodulin-binding site renders the $Na^+/H^+$ exchanger (NHE1) highly $H^+$-sensitive and $Ca^{2+}$ regulation-defective. J. Biol. Chem. **269**:13710–13715.
47. **Wakabayashi S, Fafournoux P, Sardet C, Pouyssegur J.** 1992. The $Na^+/H^+$ antiporter cytoplasmic domain mediates growth factor signals and controls "$H^+$-sensing." Proc. Natl. Acad. Sci. U. S. A. **89**:2424–2428.
48. **Wakabayashi S, Nakamura TY, Kobayashi S, Hisamitsu T.** 2010. Novel phorbol ester-binding motif mediates hormonal activation of $Na^+/H^+$ exchanger. J. Biol. Chem. **285**:26652–26661.
49. **Wakabayashi S, Pang T, Su X, Shigekawa M.** 2000. A novel topology model of the human $Na^+/H^+$ exchanger isoform 1. J. Biol. Chem. **275**:7942–7949.
50. **Wakabayashi S, Shigekawa M, Pouyssegur J.** 1997. Molecular physiology of vertebrate $Na^+/H^+$ exchangers. Physiol. Rev. **77**:51–74.
51. **Willoughby D, Masada N, Crossthwaite AJ, Ciruela A, Cooper DM.** 2005. Localized $Na^+/H^+$ exchanger 1 expression protects $Ca^{2+}$-regulated adenylyl cyclases from changes in intracellular pH. J. Biol. Chem. **280**:30864–30872.
52. **Xiang B, et al.** 2003. The catalytically active domain in the A subunit of calcineurin. Biol. Chem. **384**:1429–1434.
53. **Xue J, et al.** 2010. Elevated myocardial $Na^+/H^+$ exchanger isoform 1 activity elicits gene expression that leads to cardiac hypertrophy. Physiol. Genomics **42**:374–383.
54. **Yakel JL.** 1997. Calcineurin regulation of synaptic function: from ion channels to transmitter release and gene transcription. Trends Pharmacol. Sci. **18**:124–134.
55. **Yi YH, et al.** 2009. Membrane targeting and coupling of NHE1-integrinalphaIIbbeta3-NCX1 by lipid rafts following integrin-ligand interactions trigger $Ca^{2+}$ oscillations. J. Biol. Chem. **284**:3855–3864.
56. **Zachos NC, Tse M, Donowitz M.** 2005. Molecular physiology of intestinal $Na^+/H^+$ exchange. Annu. Rev. Physiol. **67**:411–443.